INVESTIGATION OF *Hoxa2* GENE FUNCTION IN PALATE DEVELOPMENT USING A RETROVIRAL GENE DELIVERY SYSTEM

A Thesis Submitted to the College of

Graduate Studies and Research

in Partial Fulfillment of the Requirements

for the Degree of Master of Science

in the College of Pharmacy and Nutrition

University of Saskatchewan

Saskatoon

By

Xia Wang

PERMISSION TO USE

In presenting this thesis in partial fulfillment of the requirements for a postgraduate degree from the University of Saskatchewan, I agree that the libraries of this University make it freely available for inspection. I further agree that permission for copying of this thesis in any manner, in whole or in part, for scholarly purposes may be granted by Dr.Adil J. Nazarali, who supervised my thesis work or, in his absence, by the Dean of the College of Pharmacy and Nutrition in which my thesis work was done. It is understood that any copy or publication or use of this thesis or parts thereof for financial gain shall not be allowed without my written permission. It is also understood that due recognition shall be given to me and to the University of Saskatchewan in any scholarly use which may be made of any material in my thesis.

Requests for permission to copy or to make other use of material in this thesis in whole or part should be addressed to:

Dean of the College of Pharmacy and Nutrition
University of Saskatchewan
110 Science Place
Saskatoon, Saskatchewan S7N 5C9

Abstract

Cleft palate is a common human birth defect caused by any process which interferes with palatogenesis. Studies in *Hoxa2* mutant (*Hoxa2*$^{-/-}$) mice which exhibit a secondary cleft palate were reported to be due to an abnormal positioning of the tongue which prevents normal palatal shelf fusion to occur. To obtain direct evidence for the importance of *Hoxa2* in murine palate development, an *in vitro* whole organ palatal culture model was developed, eliminating any influences from the tongue. A retroviral gene delivery system was employed, containing either *Hoxa2* sense or *Hoxa2* antisense cDNA, to respectively enhance or knockdown the expression of *Hoxa2* mRNA in the developing palate.

Our results show that palatal cultures infected with the lowest titer of *Hoxa2* sense virus induce a fusion rate of 72.7%, which is similar to palatal cultures treated with the control virus (81.8%), although fusion rates of 41.2% to 50.0% were observed in palates infected with higher titers. With the antisense virus treated group, a more profound inhibition of the fusion rate was observed (27.7% - 46.1%), which is comparable with the frequency of palatal fusion in *Hoxa2*$^{-/-}$ mice (44.4%). Additionally, the palatal shelves in both sense and antisense virus treated groups appear to be relatively shorter in length, than those measured in the control group. Interestingly, in the antisense virus treated group, the ratio of the length of the fused portion to the length of palatal shelves appears to be relatively large compared to the control group. Verification and quantification of *Hoxa2* mRNA in the developing palate between E12.5 and E15.5 was performed by real-time RT-PCR. *Hoxa2* gene expression was observed at all stages studied, with expression being the highest at E12.5 and declining from E13.5. The expression level remained constant from E13.5 through E15.5. These findings demonstrate for the first time that *Hoxa2* may play a direct role in murine palate development.

Results suggest that both factors (the absence of *Hoxa2* gene in the palate causing delayed palatal development, as well as the position of the tongue) appear to act in unison to produce cleft palate in *Hoxa2* knockout mice.

ACKNOWLEDGEMENTS

This journey began in September of 2003 and I found if I listed everyone who has taught, inspired, influenced and helped me along the way this would be several pages long. Foremost, my supervisor, Dr. Adil Nazarali – I have learned, grown and discovered so much with him over the last two years. We have turned all of this into a reality and I thank him for everything. Dr. Ronald Steer and Dr. William Waltz, who encouraged me three years ago when I took this big turn in my life, I appreciate their help very much.

Many people have contributed to my thesis in a variety of ways. I thank in particular, Dr. William Kulyk and Dr. Ed Krol, for their discussions and ideas at various points throughout the project; Dr. Marianna Foldvari and the external examiner, Dr. Bernhard Juurlink, who gave me many helpful suggestions and comments in my thesis corrections. Also, Anita Givens-Amilio, who helped in culturing the EcoPack2-293 packaging cell line, and Sandy Knowles, who helped make changes to the thesis draft just before this Christmas. Thanks to both of them. Lots of support and help from my friends: Vineeth Iyengar, Edwin Yeow and Sheng Yu, thank you for all your encouragements.

To my mother and father

献给我的爸爸, 妈妈

TABLE OF CONTENTS

LIST OF TABLES

LIST OF FIGURES

LIST OF ABBREVIATIONS

Ab/Am	Antibiotic/Antimycotic
ALK-2	Active receptor-like kinase 2
ALK-5	Active receptor-like kinase 5
Apaf	Apoptotic protease-activating factor
BA	Branchial arch
BCP	1-bromo-3-chloropropane
BCS	Bovine Calf Serum
Bmpr	Bone morphogenetic receptor
BMPs	Bone morphogenetic proteins
BSA	Bovine Serum Albumin
Cdk4	Cyclin-dependent protein kinase
cfu	colony forming units
CLP	Clefts of the secondary palate
CMV	Human Cytomegalovirus
C_T	Threshold Cycle
DEPC	Diethyl Pyrocarbonate
Dlx	Vertebrate homologue of *Drosophila* distal-less gene
DMEM	Dulbecco's Modified Eagle's Medium
DMSO	Dimethyl Sulfoxide
DNA	Deoxyribonucleic acid
DPBS	Dulbecco's Phosphate-Buffered Saline
d.p.c.	Days Postcoitum
D-V	Dorso-ventral
E	Embryonic day
ECM	Extracellular matrix
EDTA	Ethylenediaminetetraacetic Acid
EGF	Epidermal Growth Factor
EGFP	Enhanced Green Fluorescent Protein
EMT	Epitheial-mesenchymal transdifferentiation
FBS	Fetal Bovine Serum

FFP	Frequency of Fused Palates
Fgfr	Fibroblast growth factor receptor
fgfr2b	Fibroblast growth factor receptor 2b
FGFs	Fibroblast growth factors
fgf10	Fibroblast growth factor 10
GAG	Glycosaminoglycan
G418	Aminoglycoside antibiotic
GFP	Green Fluorescent Protein
Gh	greater horn of hybrid
Has	Hyaluronan synthases
Hg	hyoglossus
Hox	Clustered Antennapedia class of homeobox genes
HRP	Horse radish peroxidase
Hyal	Hyaluronidase
KCl	Potassium Chloride
KH_2PO_4	Potassium hydrogen phosphate
LEF1	Lymphoid enhancer-binding factor 1
LFP	Length of Fused Portion
LPS	Length of Palate Shelf
LTR	Left Terminal Repeat
mRNA	messenger Ribonucleic Acid
M	Mesenchyme
MCS	Multiple Cloning Site
MEE	Medial edge epithelium
MEM	Modified Eagle's Medium
MES	Midline Epithelial Seam
MMPs	Metalloproteinases
Msx	Vertebrate homologue of *Drosophila* muscle segment (*Msh*) gene
NaCl	Sodium Chloride
Na_2HPO_4	Sodium phosphate dibasic
Neo	Neomycin Resistance

NORs	Nucleolar organizer regions
PBS	Phosphate-buffered saline
PCR	Polymerase Chain Reaction
P_{CMV}	Human Cytomegalovirus (CMV) Immediate Early Promoter
r	rhombomere
r1/r2	Boundary between rhombomere 1 and rhombomere 2
R-C	Rostro-Caudal
RFPPS	Ratio of length of Fused Portion to the length of Palate Shelf
rpm	Revolutions per minute
RT	Room temperature
RT-PCR	Reverse Transcriptase Polymerase Chain Reaction
SDS-PAGE	Sodium dodecyl sulphate - polyacrylamide gel electrophoresis
Shh	Sonic hedgehog
ss	Somite stage
TE	Tris EDTA buffer
TGFβ	Transforming growth factor beta
Tgfβr2	Transforming growth factor beta receptor type II
TUNEL	Terminal deoxynucleotidyl transferase mediated nick end labeling
UNG	uracil-N-glycosylase
Wnt	Vertebrate homologue of *Drosophila* wingless gene

1. Introduction

In mouse embryos, the secondary palate initially develops bilaterally as two vertical projections (palatal shelves) from internal surfaces of maxillary prominences at embryonic day (E) 12. The two palatal shelves grow down along the sides of the tongue and subsequently elevate to become horizontally oriented above the tongue, thus allowing them to approach each other. At E14.5 the shelves meet at the midline and begin to fuse to form a single continuous palate (Ferguson, 1988). The fusion of the palatal shelves involves adhesion, migration, apoptosis, and transdifferentiation of the epithelial cells into mesenchyme (Cuervo et al., 2002; Ferguson, 1988; Griffith and Hay, 1992; Martinez-Alvarez et al., 2000b; Shuler et al., 1991; Shuler et al., 1992). Any defects of the regulation at the palate developmental stage such as timing, rate, or extent of outgrowth results in failure of the palatal shelves to fuse, and therefore causes a cleft palate (Diewert and Wang, 1992; Helms et al., 1997).

Genetic studies have revealed the involvement of numerous genes in the palate development process, including genes encoding a variety of transcription factors, growth factors and receptors (Moxham, 2003). In the developing mouse embryo, the *Hoxa2* gene has an anterior limit of expression at the rhombomere 1/ rhombomere 2 (r1/r2) boundary. Although *Hoxa2* transcripts are detected in r2, this gene is not expressed in the neural crest once these cells start to migrate from r2 into the first branchial arch (Prince and Lumsden, 1994). This results in the first branchial arch (composed of crest cells from r1 and r2 of the hindbrain and midbrain) being completely devoid of *Hoxa2* gene expression (Kontges and Lumsden, 1996). The *Hoxa2* gene appears to act as a selector gene specifying the fate of the second arch (Grammatopoulos et al., 2000). Studies using

transgenic mice suggest that *Hoxa2* null allele mice exhibit a cleft palate due to abnormal attachment of the hyoglossus muscle to the greater horn of the hyoid (Barrow and Capecchi, 1999). Ohnemus and colleagues (2001), however, found that the hyoglossus was always inserted in the hyoid of *Hoxa2-/-* mice, regardless of the presence or absence of cleft palate in *Hoxa2-/-* mice.

Hoxa2 has been found to be temporally and spatially expressed in the developing palate and appears to play a role in phenytoin-induced cleft palate (Nazarali et al., 2000). It is initially expressed in the epithelial cells of the palate primordium followed by a progressive increase in the expression levels in both epithelium and mesenchyme at embryonic day (E) 13. At E13.5, *Hoxa2* expression was the highest throughout the palatal shelf. At E14, *Hoxa2* expression was localized to the medial edge epithelium (MEE) and its presence there may serve to regulate factors involved in directing the horizontal movement of opposing palatal shelves. At E14.5, *Hoxa2* expression was visible in the developing midline epithelial seam (MES) (Nazarali et al., 2000).

These observations suggest that *Hoxa2* may play a direct role in palate formation and that the cleft palate observed in *Hoxa2* mutant *(Hoxa2*-/-) mice may not solely be due to an abnormal tongue musculature.

2. Objectives and Hypothesis

The aim of this study was to obtain further direct evidence for the role of *Hoxa2* gene in the developing murine palate. In particular, the effect of infection with *Hoxa2* sense and antisense retrovirus on palatal organ culture, and the related retrovial titer dependencies has been investigated.

My hypothesis is that altering *Hoxa2* gene expression in a mouse whole palatal organ culture model (in the absence of tongue) using a *Hoxa2* sense or antisense retrovirus will enhance or suppress *Hoxa2* expression, respectively, and will directly impact palatal development.

3. Literature review

3.1 Basic concepts of craniofacial development

3.1.1 Segmentation identity of the hindbrain

The vertebrate hindbrain is an important source of patterning information and exerts profound influences on craniofacial development. During early vertebrate embryonic development, the hindbrain becomes transiently subdivided into eight sub-units called rhombomeres (Fig. 1) (Lumsden and Keynes, 1989). Each rhombomere (r) represents a lineage-restricted compartment, showing a distinct set of molecular and cellular properties including restrictions in cell mixing. They are made up of cells that have a very early commitment to a particular developmental fate (Fraser et al., 1990) and give rise to unique regions of the mature adult brain (Birgbauer and Fraser, 1994; Fraser et al., 1990; Hunt et al., 1991b; Kontges and Lumsden, 1996; Marin and Puelles, 1995; Wilkinson, 1989; Wilkinson et al., 1989; Wintgate and Lumsden, 1996). This segmental organization of the hindbrain presages the establishment of an anatomical and functional registration between individual rhombomeres, cranial ganglia, branchiomotor nerves, and the migration pathways of cranial neural crest cells into the branchial arches (Clarke and Lumsden, 1993; Lumsden and Keynes, 1989; Sechrist et al., 1993).

The establishment of the segmental identity and the maintenance of organized patterns of gene expression during hindbrain development require the restriction of cell intermingling between adjacent segments. Cells which have similar adhesive properties such as those from odd or even rhombomeres display a preferential association (Guthrie and Lumsden, 1991; Guthrie et al., 1993). The appearance of restricted domains of gene expression in the hindbrain coincides with r partitioning and the adoption of the specific

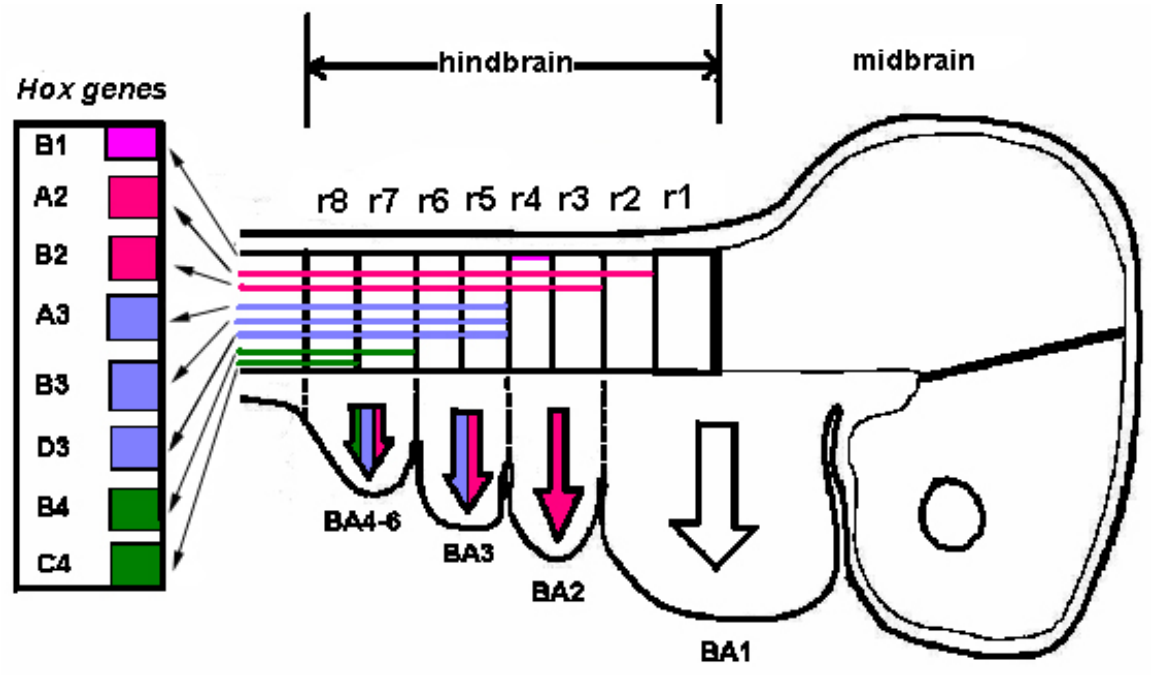

Figure 1 *Hox* gene expression in rhombomeres (r) and migrating neural crest. Branchial arch 1 (BA1) is populated with neural crest cells from the posterior midbrain and r1/r2, none of these migrating crest cells express *Hox* genes. BA2 is populated with neural crest cells from r4 (with minor contributions from r3 and r5) and expresses *Hoxa2*. BA3 is populated by neural crest cells from r6 with minor contributions from r5 and r7, these cells express *Hox* genes from paralogous groups 2 and 3 (Redrawn from Cobourne, 2000).

neural characters. Numerous genes including transcription factors, signaling molecules, membrane and nuclear receptors are dynamically expressed in segmentally restricted patterns during hindbrain development. Some genes are expressed in single rhombomeres (Lumsden and Krumlauf, 1996; Trainor et al., 2000; Wilkinson, 1995)

3.1.2 The role of neural crest cells

The neural crest is a highly pluripotent cell population that plays a critical role in patterning the vertebrate head (Cobourne, 2000). In the vertebrate, neural tissue is induced in the ectoderm of the embryo at the earliest stage of neural development. As a result of neural induction, the ectoderm is then divided into three different regions: the neural ectoderm or neural plate, the non-neural ectoderm which will form epidermis, and the cells at the border between neural and non-neural ectoderm which for the most part will become the neural crest cells. During neurulation, the neural plate border bends to form the neural folds and eventually gives rise to the dorsal aspect of the neural tube (Gammill and Bronner-Fraser, 2003) (Fig.2).

In the developing head, the cranial neural crest migrates from the posterior midbrain and hindbrain regions into the branchial arch system. The cranial neural crest cells then interact with epithelial and mesodermal cell populations within the arches, leading to the formation of craniofacial bones, cartilages and connective tissues (Cobourne, M., 2000). The neural crest cells that migrate and form the bulk of the facial mesenchyme originate from the same axial level of the neural tube. Neural crest cells destined for the first branchial arch migrate essentially from r 1 and 2, while those for the second and third arches migrate from r 4 and 6, respectively (Fig. 1). The even numbered rhombomeres (2, 4, and 6) contain the exit points for cranial nerves V, VII, and IX, nerves that will

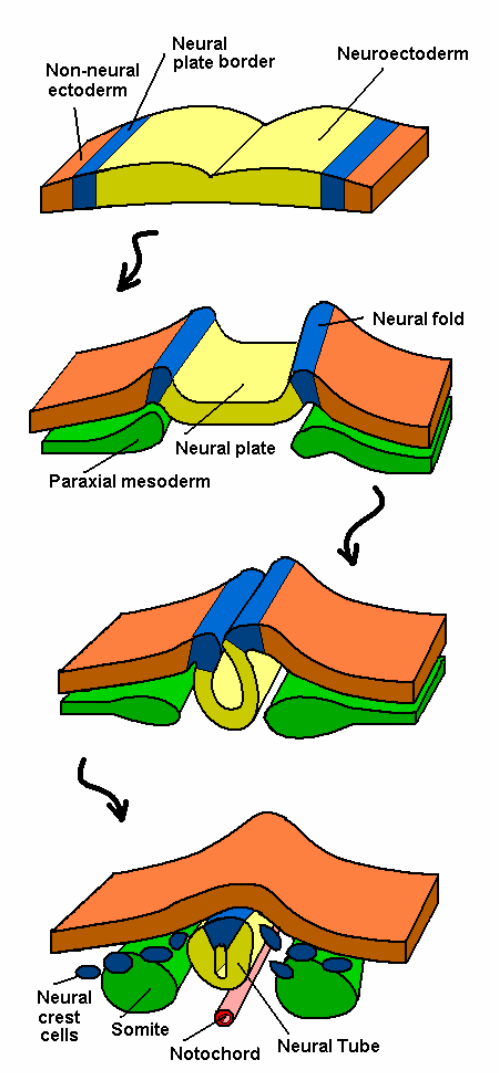

Figure 2 Neural border induction and neurulation. The neural plate border (blue) is induced by signaling between the neuroectoderm (yellow) and the non-neural ectoderm (orange) and from the underlying paraxial mesoderm (green). During neurulation, the neural plate borders (neural folds) bend, causing the neural plate to roll into a neural tube. Neural crest cells (blue) delaminate from the neural folds or the dorsal neural tube, depending on the species and axial level (Redrawn from Gammill and Bronner-Fraser, 2003).

innervate branchial arches 1, 2, and 3. This leads to the concept that an axial-level specific body code is established when the neural crest cells form part of the neural plate. After neural crest cells' migration into the branchial arches, individual structures within the arches begin to develop that eventually form a composite head structure such as face, tongue, lips, jaws, palate pharynx and neck (Cobourne, 2000).

3.1.3 Migration and segregation of cranial neural crest cells

The cranial crest cells do not migrate as a single mass, instead, they are organized into streams, three of which can be identified in the developing head of all vertebrate embryos: trigeminal, hyoid, and post-otic (Graham et al., 2004). These three streams populate the first, second and third branchial arches respectively, in keeping with their craniocaudal axial origins (Lumsden et al., 1991) and give rise to a great extent of cell lineages, which are distinct for each branchial arch (Kontges and Lumsden, 1996; Noden, 1983a) (Fig.1). The mechanism that is used to pattern the migration and segregation of cranial neural crest cells into discrete streams in the vertebrate head is essential for keeping *Hox* expressing and non-*Hox* expressing neural crest cells separated from each other (Grammatopoulos et al., 2000; Pasqualetti et al., 2000). Therefore, the streaming of the crest could act to guarantee the faithful transfer of patterning information from the neural primordium to the periphery (Graham et al., 2004). It also ensures that first arch crest, carrying cues for jaw development, would not intermingle with hyoid crest, carrying cues for the patterning of the second arch. This is a pre-requisite for proper jaw formation and a normal face development.

3.1.4 Pre-programming model of cranial neural crest cells and *Hox* genes

3.1.4.1 Homeobox genes

Homeobox genes encode transcription factors which act as regulators of downstream gene activity and are characterized by the presence of a highly conserved 180-base pair sequence called the homeobox. The homeobox encodes a 60-amino acid helix-loop-helix DNA binding motif within the transcription factor. In the fly, homeotic genes are predominantly clustered in two regions (*Antennapedia* and *bithorax*) on chromosome 3, which together make up the single *HOM-C* complex (Cobourne, M. 2000). *Hox* genes are homologous to homeotic genes of *Drosophila,* which map to the *Antennapedia* and *bithorax* complexes, are organized into a single chromosomal cluster in invertebrates, in contrast to higher vertebrates such as the mouse which have 39 *Hox* genes, organized into four distinct chromosomal clusters (*Hoxa-Hoxd*) located on different chromosomes (McGinnis and Krumlauf, 1992). This arrangement arose during evolution from a single ancestral homeobox as a consequence of duplication and divergence (Kappen et al., 1989). The most significant feature of the organized expression of *Hox* gene family members is the spatial and temporal colinearity, which confers positional information along the body axis (Dolle et al., 1989; Duboule and Dolle, 1989; Kessel and Gruss, 1991; McGinnis and Krumlauf, 1992). Genes located nearer to the 3' end of the cluster are expressed earlier, and more anteriorly than those located nearer the 5' end during development, so that *Hox* genes exhibit nested domains of expression along the anterior-posterior (A-P) axis along the neural tube and, each gene has a characteristic segmental limit of expression at its anterior boundary. They are expressed from the anterior region of the hindbrain through the length of the spinal cord (Hunt et al., 1991a) (Fig.3).

The patterns of expression of these genes show a very precise spatial restriction. In the developing head, this expression pattern is seen in the hindbrain with the anterior limits

of *Hox* gene corresponding to r boundaries at two-segment intervals. As the neural crest migrates from the r into specific branchial arches, it retains the particular combination of *Hox* gene expression that is characteristic of the r from which neural crest originates. Thus, the neural crest from each axial level of neural tube carries a unique combinatorial *Hox* gene code (Fig.1). This code can be considered to specify pattern and formation of the different branchial arch derived tissues of the head and neck. Interestingly, the first branchial arch from which the maxillary and mandibular processes develop does not express *Hox* genes (Hunt and Krumlauf, 1991). However, subfamilies of homeobox genes which are more diverged from the ancestral *Hox* genes, such as *Msx1*, *Msx2* (MacKenzie et al., 1991), the *Dlx* family (Qiu et al., 1997; Qiu et al., 1995), *Mhox* (Cserjesi et al., 1992) and *Goosecoid* (Gaunt et al., 1993), are found to be spatially expressed within the first branchial arch.

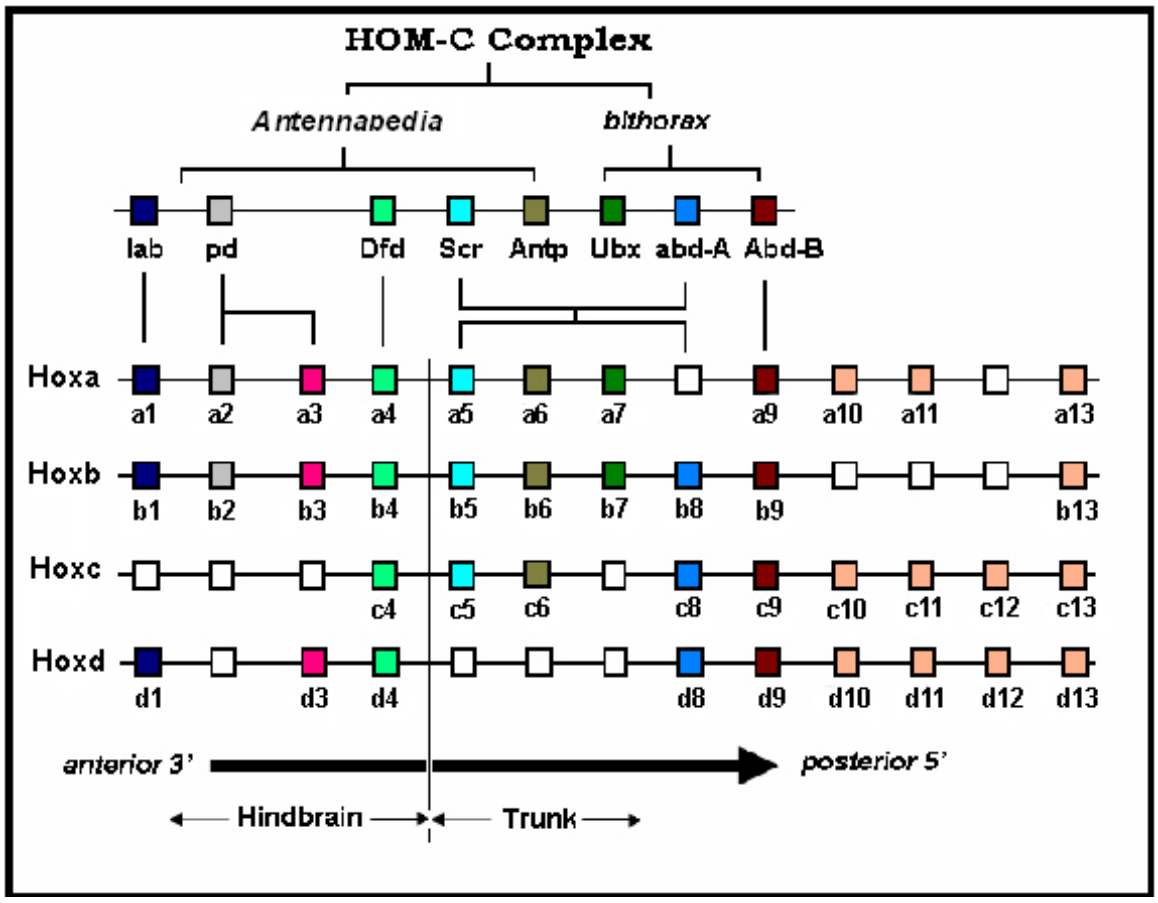

Figure 3 The 39 mouse *Hox* genes are organized in four clusters on four chromosomes. They are derived from a single ancestral cluster from which the single *HOM-C* complex in *Drosophila* is also derived. *HOM-C* consists of two regions: *Antennapedia* and *Bithorax*. Cluster duplication during evolution has led to the concept of paralogous groups of *Hox* genes. Groups of up to four genes derived from a common ancestral gene can be identified based upon sequence homology. The paralogues show similar expression domains along the anterior-posterior axis of the embryo leading to the concept of functional redundancy between genes (Redrawn from Cobourne, 2000).

3.1.4.2 Pre-programming model of cranial neural crest cells

The generation of regional diversity in the vertebrate head is believed to be a consequence of patterning information provided by migrating neural crest cells and, neural fold transplantation experiments have provided much of the basis of our current understanding of the role of neural crest in craniofacial patterning (Andres, 1949; Noden, 1983; Wagner, 1959). When first arch (mandibular) neural crest cells were grafted posteriorly in second (hyoid) or third (visceral) arch neural crest, the transplanted neural crest cells formed duplicated first arch skeletal elements (Noden, 1983). This suggested firstly, that neural crest cells may be pre-programmed prior to their migration from the neural tube to branchial arches and secondly, that myogenic populations and other cell types can receive spatial cues from the invading neural crest-derived connective tissues. The majority of cranial neural crest cells are derived from the hindbrain. Investigations have showed that the same restricted domains of *Hox* gene expression in the hindbrain are followed in the migrating neural crest cells, and then later in the ganglia and branchial arches (Hunt et al., 1991a). Under this preprogramming model, it was believed that positional information encoded by the *Hox* genes was carried passively by the neural crest cells from the hindbrain to peripheral tissues and branchial arches, where it was elaborated to develop the characteristic head structures. Therefore, it was hypothesized that the spatial organization of structures within the vertebrate head was determined by the neural crest and furthermore that the positional information carried by the neural crest was irreversibly determined before the neural crest migrates from the neural tube (Trainor, 2003a).

3.1.5 Cranial neural crest plasticity and its limitations

Two interesting features have been revealed concerning the role of *Hox* genes in patterning cranial neural crest derivatives. First, it has been shown that in the chick and frog, if expression of *Hoxa2* is experimentally induced in all branchial arch 1 tissues such as in the ectoderm, neural crest, mesoderm and endoderm of the first branchial arch, a partial homeotic transformation of branchial arch 1 into branchial arch 2 is observed (Grammatopoulos et al., 2000; Pasqualetti et al., 2000). In contrast, if *Hoxa2*, *Hoxa3* or *Hoxb4* are individually expressed into the rostral expression domain of the cranial neural crest, the ability of these neural crest cells to differentiate into skeletal structures is abolished, completely for *Hoxa2*, and partly for *Hoxa3* and *Hoxb4* (Creuzet et al., 2002). Therefore, the environment in which these neural crest cells develop is crucial for specifying their fates, and *Hox* genes appear to have an important role to play.

Recently, there have been significant advances in our understanding of craniofacial patterning through neural crest cell transpositions within the hindbrains of mouse (Golding et al., 2000; Trainor and Krumlauf, 2000) and zebrafish embryos (Schilling et al., 2001). In contrast to the classic analyses carried out in avian embryos, these new studies revealed a consistently high degree of cranial neural crest cell plasticity. In heterotopic transplantations of neural crest cells within mouse and zebrafish hindbrains, graft derived neural crest cells migrate into the nearest arch without any evidence of path finding and inappropriate downregulating of *Hox* gene expression in these cells (Trainor and Krumlauf, 2000). In zebrafish embryos, it was found that these transplanted cells activated new processes of gene expression, and they differentiated and gave rise to the pharyngeal cartilages appropriate to their new axial location (Schilling et al., 2001).

These results indicate that the characteristics of cranial neural crest cells are neither fixed nor passively transferred from the hindbrain to the branchial arches and the periphery of the head. The plasticity observed in neural crest cell patterning correlates with molecular analyses that have identified distinct cis-regulatory elements controlling *Hox* gene expression in different tissue such as the neural tube and neural crest (Maconcochie et al., 1999). This implies that neural crest cells can respond and adapt to the environment in which they migrate, and furthermore, the cranial mesoderm plays an important role in patterning the identity of the migrating neural crest cells (Golding et al., 2000).

More importantly, these new findings for neural crest plasticity and independent gene regulation can be reconciled with the classic studies to promote a neural crest pre-programming model. The differences in the degree of plasticity observed in mouse and zebrafish embryos, when compared with avians, can be partially accounted for by the cell community, such as the size of the transplanted tissue, and the stage at the time of transplant (Trainor and Krumlauf, 2000). For instance, when whole hindbrains and pairs of rhombomeres are transplanted, inter-rhombomeric signaling and neighbouring cell signaling can help to reinforce and maintain the identity of the transplanted cells. However, in the case of small sub-rhombomeric cell populations (mouse and zebrafish) and single cells (zebrafish), the transplanted cells lack this neighbouring reinforcement. The graft-derived neural crest cells migrate as a dispersed population and, therefore, are more likely to respond to the new environment in which they migrate (Trainor et al., 2002).

3.2 Craniofacial development

3.2.1 The initial development of the face

It is apparent that the postnatal vertebrate head exhibits an extremely intricate and varied morphology. Initially, however, the craniofacial complex has a much simpler geometry, comprised of a series of swellings or prominences that subsequently grow, meet and fuse (Helms et al., 2005). During early embryonic development, there are seven prominences that constitute the vertebrate face: the frontonasal prominence and three paired prominences derived from the first branchial arch (Helms et al., 2005). The proliferation of the underlying mesenchyme of the lower part of the frontonasal prominence creates prominent elevations, the medial and lateral nasal processes. The medial nasal process forms the forehead, the middle of the nose, the upper lip and the primary palate, while the lateral nasal process form the sides of the nose (Larson, 2001). The major ventral region of the first branchial arch gives rise to the paired mandibular prominence and forms the lower jaw. The dorsal portion of the first branchial arch gives rise to paired maxillary prominences that form the sides of the middle and lower face, the lateral borders of the lips, and the secondary palate (Fig.4).

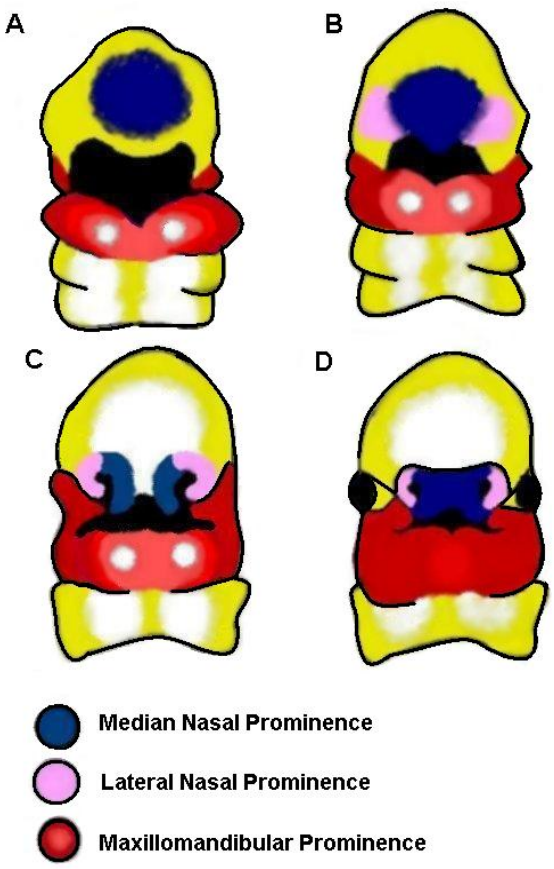

Figure 4 Development of the craniofacial primordial (A-D). A frontal view of the prominences that form the main structures of the face. The frontonasal (or median nasal) prominence (blue) contributes to the forehead (A), the middle of the nose (B), the philtrum of the upper lip (C) and the primary palate (D), while the lateral nasal prominence (pink) gives rise to the sides of the nose (B,D). The maxillomandibular prominences (red) form the lower jaw (specifically from the mandibular prominences), to the sides of the middle and lower face, to the lateral borders of the lips, and to the secondary palate (from the maxillary prominences) (Redrawn from Helms et al., 2005).

3.2.2. Identity of the first branchial arch

In most vertebrates, branchial arches are segmental structures of the embryonic neck which are transformed into many derivatives during embryonic development. Branchial arch identity is established by expression of a unique combination of homeobox genes (Gendron-Maguire et al., 1993; Mallo and Brandlin, 1997; Rijli et al., 1993; Schneider and Helms, 2003; Trainor and Krumlauf, 2000; Trainor and Krumlauf, 2001). The subepithelial mass of the first branchial arch is populated by neural crest cells migrating from the posterior midbrain through to the r 2. These migrating neural crest cells do not exhibit *Hox* gene expression (Francis-West et al., 2003; Hunt et al., 1998b; Hunt and Krumlauf, 1991; Richman and Lee, 2003), unlike more caudal neural crest cells that migrate into branchial arches 2 to 6 (Hunt et al., 1998b; Irving and Mason, 2000; Noden, 1983; Prince and Lumsden, 1994; Trainor et al., 2002).

After the migration of neural crest cells, the first branchial arch consists of the ectodermal epithelium of stomodeum (primitive oral cavity), the primitive gut endoderm after the pharyngeal membrane and the surface ectodermal epithelium (future skin). It also comprises of neural crest derived ectomesenchyme (Chai et al., 2000; Noden, 1986; Noden, 1988; Trainor and Tam, 1995) and a small portion of central mesenchymal core which may be derived from the original mesodermal cells within the first branchial arch (Francis-West et al., 2003). Both mesenchymal components are combined during further development of the facial skeleton, musculature and other connective tissues, involving many signaling pathways to establish the axial polarity and /or segmentation of developing tissues (Dudas and Kaartinen, 2005).

3.2.3 Patterning contributions from neural crest cells

The cranial neural crest cells are derived from the neural tube between the midbrain and the 4th somite, and are responsible for the generation of a diverse range of craniofacial tissues. The majority of the facial skeleton is constructed from neural crest cells that originate from the axial level between the midbrain and r 1 and 2 (Lumsden et al., 1991), which enter the frontonasal prominence and first branchial arch, while individual prospective facial prominences are populated from specific axial levels within the mid-and hindbrain. The neural crest enter these transient embryonic structures as an anatomically unpatterned population (Farlie et al., 2004).

The contributions of the neural crest to facial patterning were determined by exchanging neural crest cells between ducks and quails (Schneider and Helms, 2003), which showed the grafted crest cells maintained the morphogenetic program of the donor species, regardless of mesodermal, endodermal, and ectodermal morphogenetic influences from the host (Farlie et al., 2004). Recently, Tucker and Lumsden (Tucker and Lumsden, 2004) found that the neural crest has an inherent property to determine species-specific skeletal elements in the face, and concluded that this characteristic is generated in response to signals from epithelia. Furthermore, the extent to which facial features were transformed in both these experiments was directly proportional to the number of transplanted neural crest cells that made these tissues, which showed a "population-dependent" manner in the transformation (Helms et al., 2005), which can also be partially accounted for by the cell community, such as the size of the tissue transplanted and timing effects (Trainor and Krumlauf, 2000).

3.2.4 Pharyngeal endoderm in facial skeleton morphogenesis

That the pharyngeal endoderm plays a role in facial skeleton development became apparent when defined regions of endoderm were surgically removed from 5-6 somite stage (ss) chick embryos, resulting in the absence of facial skeletal elements (Couly et al., 2002). With this approach, defined areas of the endoderm were identified as being necessary for the development of the nasal septum, Meckel's cartilage, articular and quadrate cartilages, and the anterior part of the hyoid complex. These findings were also confirmed when strips of pharyngeal endoderm were grafted from stage-matched quail embryos into the migration pathway of cranial neural crest cells in chick, causing the duplication of the corresponding skeletal elements. The extra cartilages that formed in contact with the quail endoderm were made up of chick cells, meaning that they resulted from the induction of the host neural crest cells by the grafted endoderm. The response found in avian embryos was a remarkable duplication in pharyngeal arch skeletal structure, which was the general morphology correlated with the level from which the endodermal graft was derived (Ruhin et al., 2003).

Further experiments also showed that, in addition to being essential for shaping cartilage rudiments, signals from the ventral forgut endoderm dictate the position that is adopted by facial cartilages with respect to the body axis (Couly et al., 2002). *Hox*-expressing neural crest cells are similarly responsive to endodermal cues arising from the more caudal part of the foregut endoderm (Ruhin et al., 2003). Experiments demonstrate that pharyngeal endoderm has a profound influence on the morphogenesis of the middle and lower face (Crump et al., 2004a; Crump et al., 2004b; Trokovic et al., 2003; Veitch et

al., 1999). Recent work shows that FGF signaling is essential for this tissue patterning (Crump et al., 2004a).

3.3 Development of the secondary palate

3.3.1 Introduction

In humans, the secondary palate develops between the sixth and eighth week of intra-uterine life (Berkovitz et al., 2002; Ferguson, 1978; Johnston and Sulik, 1990; Sadler, 2000). During the sixth week, the palatal processes develop from the oral aspect of the first arch maxillary processes as downward-directed projections. They grow laterally behind the primary palate and this process continues such that they come to lie vertically by the seventh week of development. The tongue occupies the space between the two processes and fills the oronasal cavity. During the eighth week of development, the tongue "drops" and the vertically-inclined palatal shelves become horizontal. On becoming horizontal, the two palatal shelves contact each other in the midline. After contact, the medial edge epithelia (MEE) of palatal shelves fuse to form a "midline epithelial seam" (MES). Subsequently, this epithelial seam degenerates so that mesenchymal continuity is established, forming an intact secondary palate (Moxham, 2003). Fusion of the palatal shelves occurs first in the region of the second ruga (middle third of the palate) from which point fusion spreads anteriorly and posteriorly (Ferguson, 1988). Fusion with the posterior surface of the primary palate and the lower free edge of the nasal septum separate the nasal and oral cavities. In humans, this is complete by the twelfth week of development (Moxham, 2003).

3.3.2 Overview of secondary palate development in animal kingdom

In birds, amphibians and some reptiles, the bilateral palatal shelves that arise from the maxillary processes initially develop and grow horizontally above the dorsum of the tongue (Ferguson et al., 1984; Ferguson and Honig, 1985; Koch and Smiley, 1981; Shah et al., 1985; Shah et al., 1987; Shah and Crawford, 1980). The horizontal shelves approximate and contact each other, but their MEE never adhere or fuse, resulting in a permanent cleft palate (Koch and Smiley, 1981; Ferguson et al., 1984; Ferguson and Honig, 1984; Ferguson and Honig, 1985; Shah et al., 1985; Shah et al., 1987). However, one group of reptiles, the crocodilians, develop a fused mammal-like secondary palate (Ferguson, 1981a; Ferguson, 1981b; Ferguson and Honig, 1984; Ferguson and Honig, 1985). In alligators and crocodiles, upon contact, the MEE of the palatal shelves show a very restricted region of adherence, fusion and cell death near the oral edge. The shelves then establish mesenchymal continuity by a merging process with mesenchymal infilling and migration of the MEE into the nasal aspect of the palate (Ferguson, 1981a; Ferguson and Honig, 1984; Ferguson and Honig, 1985). Thus, a fused epithelial seam with medial edge cell death is not a feature of alligator secondary palate development. Secondary palate development appears to be absent in lower vertebrates including fish. An initial vertical growth of the palatal shelves is peculiar to mammals. MEE cell adhesion, fusion to form a seam and subsequent cell death with an intact palate, are also the only characteristics found in mammals (Ferguson et al., 1984).

3.3.3 Origin of the mesenchyme contributing to palate development

Within the palatine processes, the origin of the mesenchyme contributing to the development of palate is derived from neural crest cells (Couly et al., 1992; Kontges and Lumsden, 1996; Le Douarin and Kalcheim, 1999; Noden, 1978). Been and Song (1978)

have shown that localized destruction of midbrain neural crest interferes with palatal closure. Recent work suggests that craniofacial development does not completely depend on neural crest pre-programming but is controlled by a complex combination of cell and tissue interactions (Trainor and Krumlauf, 2001), which suggests that neural crest cells can be reprogrammed and their fate and identity depend upon the surrounding tissue environments and cellular signals they receive as they migrate to their target locations (Schilling et al., 2001). This seems to be occurring as a result of alteration in *Hox* gene identity (Grammatopoulos et al., 2000; Pasqualetti et al., 2000).

3.3.4 Palatal shelf elevation

The mechanisms responsible for mammalian palatal shelf elevation are complex. On the one hand it involves the generation of an internal shelf-elevating force and on the other, it may be due to developmental changes in the surrounding face. Several mechanisms have been proposed to account for the rapid movement (Brinkley, 1980; Ferguson, 1978) of the palatal shelves from the vertical to the horizontal position, however, the source of the forces responsible for palatal shelf reorientation/elevation is a matter of controversy. It has been proposed that the intrinsic shelf elevation force might develop as a result of hydration of extracellular matrix (ECM) components, principally hyaluronan, in the shelf mesenchyme (Brinkley and Morris-Wiman, 1984; Brinkley and Morris-Wiman, 1987; Ferguson, 1978; Larsson et al., 1959; Pratt et al., 1973; Singh et al., 1997; Singh et al., 1994), or as a result of mesenchymal cell activity (Babiarz et al., 1979; Brinkley and Bookstein, 1986; Bulliet and Zimmermann, 1985; Innes, 1978; Luke, 1984; Shah, 1979; Shah et al., 1989; Shah and Crawford, 1980; Wee et al., 1979; Zimmerman, 1979).

Much recent work has focused on the changes in the ECM of the palatal shelf's mesenchyme during palate shelf elevation. Singh et al. (1994) has reported significant changes in glycosaminoglycans (GAG) after palate shelf elevation in rats. Three types of GAG are found in the developing palatal shelves in vivo: hyaluronan, heparan sulphate and chondroitin-4-sulphate (Singh et al., 1997; Singh et al., 1994) and much attention has focused on the role of hyaluronan in shelf elevation. Hyaluronan is highly electrostatically charged, displaying non-ideal osmolarity, and its open coil structure enables it to bind up to 10 times its own weight in water (Brinkley and Morris-Wiman, 1987; Pratt et al., 1973). It has been proposed that hyaluronan is a GAG involved in shelf elevation, and this was supported by the observation of an increase in water content of the palatal shelves up until shelf fusion (Foreman et al., 1991). Other studies (Thomas, 1999) have revealed the presence of the enzyme hyaluronidase, that degrades hyaluronan and affects palatogenesis in an organ culture. That palates treated with this enzyme produced cleft palates indicating that palate development is disrupted in the absence of hyaluronan. Other than hyaluronan, a set of macromolecules generated in the Golgi complex may also play an important role in normal palate development as the presence of Brefeldin A, a drug which inhibits vesicular transport through the Golgi complex, produced a cleft palate in vitro.

Other recent studies implicate hyaluronan binding protein splice variants of CD44, versican and RHAMM and isoforms of hyaluronan synthases (*Has*) and hyaluronidases (*Hyal*) in the rat developing palate (Itano et al., 1999). The major hyaluronan binding protein CD44 was found to display both transient and dynamic expression during shelf elevation. Expression of Both *Has* and *Hyal* enzymes is necessary during palate

development as they can produce different sizes of hyaluronan, thus promoting distinct cellular responses in different cell types (Itano et al., 1999). Small chains of hyaluronan can induce gene expression (McKee et al., 1996), cell signaling responses and cell differentiation (Termeer et al., 2000) and cell proliferation and growth (Bourguignon et al., 1997; Mohapatra et al., 1996), while large hyaluronan chains inhibit cell growth and induce cell adhesion and migration (Noble et al., 1998). Versican splice variants are thought to form bridges, helping to stabilize the ECM and create the necessary turgor pressure to enable shelf elevation.

Other ECM components, including proteoglycans, also probably have important functional implications with shelf elevation, although its aggregation and disaggregation occurring at different regions of the palate shelf and different stages is unknown. Collagen fibres have been suggested either to direct the shelf elevation force (Bulliet and Zimmermann, 1985) and/or contribute to a critical volume of the shelves necessary for their re-orientation (Ben-Khaial and Shah, 1994).

The role of the mesenchymal cells in the palatal shelves has also been controversial. It has been suggested that a critical number of cells are required for palatal shelf elevation to occur (Shah et al., 1989), however, there is no reliable evidence as yet that these cells, by their rapid division and proliferation or by their migration or contraction, can generate a palatal shelf elevation force. It has been showed that shelf re-orientation is accompanied by changes in mesenchymal cell density and distribution (Brinkley and Bookstein, 1986). They suggested that high local cell densities were enhanced by cell division but the decreased cell density was probably related to displacement of cells caused by the ECM expansion (Brinkley and Bookstein, 1986). Ferguson (1978) also indicated a closely

packed nature of palate shelf mesenchymal cells before elevation and a greater cell density within the posterior areas of palate shelves, a region which is the last to fuse.

In addition to mesenchymal cell proliferation, the formation of a shelf elevation force might also result from changes in cellular morphology at the critical time (Brinkley and Bookstein, 1986) and particularly, from changes in the intracellular microfilamentous and microfibrillar systems (Kuhn et al., 1980). Babiarz et al (1979) reported that before elevation, palatal shelf mesenchymal cells undergo elongation and polarization. The cells nearest the basement membrane are perpendicularly aligned to the membrane. After shelf elevation, these cells become more rounded with short cellular projections. Babiarz et al (1979) suggested that these changes in cellular morphology are indicative of cell contraction that could be the means of generating the shelf elevation force. Moreover, they also reported the presence of microfilaments and suggested that these were associated with cell migration that could be responsible for shelf elevation (Babiarz et al., 1979). Wee and Zimmermann (1980) reported that cytochalasin B prevents palate shelf elevation by disrupting actin crosslinking in the cytoskeleton. However, they also found that curare (a microfilament antagonist) enhanced shelf elevation *in vitro*, thus providing evidence against the notion that microfilamentous systems are responsible for shelf re-orientation. Furthermore, it is not clear whether changes in the palate shelf mesenchymal cells are primarily related to the palate shelf re-orientation or whether they affect cell displacements/cell activities caused by changes in the ECM during palate shelf re-orientation (Pratt et al., 1973).

There have been many qualitative studies of the palate shelf mesenchymal cells with electron microscopy (Babiarz et al., 1975; De Angelis and Nalbandian, 1968; Innes, 1978)

(Ferguson, 1981a; Innes, 1981; Innes, 1985). Essentially, these studies show that the mesenchymal cells appear to be very active, possessing many mitochondria, abundant cisternae of endoplasmic reticulum, a well-developed Golgi complex, and large numbers of glycogen particles (organelles appropriate for cells actively synthesizing and secreting ECM proteins). The mesenchyme was found to be tightly packed with polygonal cells possessing centrally placed ovoid nuclei with prominent nucleoli (Lieb and De Paola, 1981). Lieb and De Paola (1981) also observed that there was a large complement of free ribosomes and polysomes and very little intercellular space. Recently, it has been reported that filopodia-like structures appear on the surface of palatal shelf cells at the time of fusion (Taya et al., 1999).

It is obvious that, whether or not the palatal shelf mesenchymal cells are involved in the generation of the shelf elevation force, these cells have to participate in events occuring in the palate shelf ECM. Using silver staining techniques to highlight nucleolar organizer regions (NORs) has confirmed that the rate of protein synthesis during palatogenesis is high, and it is higher before elevation than after elevation, and is higher still during later stages of histogenesis (Singh and Moxham, 1993).

Developmental changes in facial dimensions also help create a favorable environment for fusion to take place. Three-dimensional analyses of facial growth suggest that differential cranial growth contributes to secondary palate formation by progressively displacing the tongue downward and forward in the oronasal cavity. Also, during the period of shelf elevation, there is almost no growth in head width, but constant growth in head height (Diewert, 1978; Diewert, 1983). The predominantly sagittal growth direction

of Meckel's cartilage also appears to contribute actively to the displacement of the tongue via the attachment of the genioglossus muscle (Diewert, 1980).

3.3.5 Fusion of the palatal shelves

Once the palatal shelves have elevated, they contact each other, initially in the middle third of the palate (Ferguson, 1988) and subsequently adhere by means of an "adhesive" glycoprotein that coats the surface of the medial edge epithelium (MEE) of the shelves (Greene and Kochhar, 1974; Greene and Pratt, 1977; Pratt and Hassell, 1975; Souchon, 1975). Moreover, the epithelial cells develop desmosomes (De Angelis and Nalbandian, 1968; Morgan and Pratt, 1977) and consequently an epithelial seam is formed (Morgan and Pratt, 1977; Ferguson, 1988). Palatal fusion is a process that requires the adhesion of the MEE of each shelf and the degeneration of the resulting MES. During recent decades, this process has been very intensely studied and, in conjunction with significant improvements in the fields of molecular biology, mouse and human genetics and bioimaging, has generated a wealth of information about the physiology of normal palatogenesis, as well as information about the pathogenetic mechanism of cleft palate (Dudas and Kaartinen, 2005).

The critical step in palatal fusion is removal of MEE cells from the midline seam. Three different cell fates have been developed to account for the disappearance of the MEE from the palatal midline: programmed cell death (apoptosis), epithelial to mesenchymal transdifferentiation (EMT) and epithelial migration (Dudas and Kaartinen, 2005).

3.3.5.1 Apoptosis

The original hypothesis of apoptosis of the MEE was suggested several decades ago by a number of investigators (Farbman, 1968; Glucksmann, 1965; Pourtois, 1966; Saunders, 1966; Shuler, 1995). During recent years, new analytical tools have played a fundamental role in revealing the role of apoptosis in midline palatal fusion. First, the TUNEL assay has verified that there are positively staining cells in the midline seam, particularly in the oral-middle-nasal epithelial bordered triangle regions (Mori et al., 1994; Taniguchi et al., 1995). These studies were recently extended by Martinez-Alvarez et al. (2000b), who suggested that *TGF-β3* has a role as an inducer of apoptosis, and later by Cuervo and colleagues, showing that retinoids play a key role in induction of apoptosis in the MEE (Cuervo and Covarrubias, 2004; Cuervo et al., 2002). In addition, *in vivo* study provided by Yoshida et al. (1998), demonstrated that mice deficient in *Apaf-1* develop a *TGF-β3*$^{-/-}$ mice-like palatal phenotype, in which fully grown palatal shelves fail to fuse due to a failure of MEE cells to die. Furthermore, a recent investigation by Nawshad et al. (2004) suggested that only the outer layer of the MEE, called the periderm, undergoes apoptosis, whereas the basal MEE cells undergo EMT.

3.3.5.2 Epithelia migration and epithelial to mesenchymal transdifferentiation

Lineage tracing using membrane-intercalating vital dye, DiI, has been applied to study MEE fate in mouse palates both *in vitro* (Carette and Ferguson, 1992; Fitchett and Hay, 1989; Shuler et al., 1991) and *in vivo* (Shuler et al., 1992). Carette and Ferguson (1992) demonstrated that MEE cells migrate to oral and nasal epithelial triangles, however, Fitchett and Hey (1989), and Shuler et al. (1992), showed that during palatal fusion a large portion of MEE cells undergo a transdifferentiation from epithelial to mesenchymal cells (EMT). These conclusions have been supported by immunostaining for epithelial

and mesenchymal markers (Shuler et al., 1991, 1992). In addition, later lineage-tracing studies using green fluorescent protein in conjunction with retroviral or adenoviral gene transduction demonstrated a consistence with these original findings, showing that EMT occurs in the basal layer of the MEE (Cuervo et al., 2002; Martinez-Alvarez et al., 2000b). However, either the molecular induction mechanism of this process during palatogenesis, or how it is coordinated with apoptotic cell death is currently unknown (Dudas and Kaartinen, 2005).

3.3.5.3 TGF-β3 superfamily signaling in palatogenesis

All three mammalian *TGF-β* isoforms are found to be expressed in the palatal region before and during palate fusion. *TGF-β3* is first found to be expressed in the epithelial tips of vertically growing shelves. Its expression is then very strong in the MEE of apposing shelves and in the midline seam, but ceases simultaneously with the disappearance of the midline seam. In contrast, *TGF-β2* is expressed in the palatal mesenchyme during palatal shelf growth, elevation and fusion, whereas the pattern of *TGF-β1* is more diffuse both in the mesenchyme and later in the epithelium (Fitzpatrick et al., 1990; Pelton et al., 1990a; Pelton et al., 1990b).

It has been reported that *TGF-β3*$^{-/-}$ mutant mice suffer from isolated cleft palate without any other craniofacial symptoms (Kaartinen et al., 1995; Proetzel et al., 1995). Some studies have suggested that *TGF-β3* specifically induces EMT (Kaartinen et al., 1997; Sun et al., 1998a; Sun et al., 1998b), and other researchers have shown that *TGF-β3* induces specific cell morphological changes in the MEE (Gato et al., 2002; Martinez-Alvarez et al., 2000a; Taya et al., 1999; Tudela et al., 2002). These morphological changes include the formation of long filopodia on the apical surface of the apposing

epithelia, expression of chondroitin sulfate proteoglycan on the apical surface of the MEE, and emergence of bulging or protruding cells, which were considered that may be critical for palatal adhesion and intercalation of apposing shelves and for subsequent apoptosis (Gato et al., 2002; Taya et al., 1999; Tudela et al., 2002).

Some studies have also shown that TGF-β3 regulates expression of matrix metalloproteinases (MMPs), especially MMP-13, which plays an important role in the remodeling of the basement membrane during palatal fusion (Blavier et al., 2001). Dudas et al (2004) demonstrated recently that TGF-β3 signaling in the MEE is regulated mainly by the TGF-β type I receptor, ALK-5 (Active receptor-like kinase 5) which subsequently activates the intracellular signal transducer Smad2. Also, it was recently reported that *TGF-β3* signaling is capable of activating the *LEF1* (Lymphoid enhancer binding factor 1) gene in the MEE (Nawshad and Hay, 2003), however, this activation of LEF1 was found to be Smad2-dependent without involving β-catenin. This is rather surprising, as TGF/LEF1 transcription factors are usually activated by the canonical Wnt/β-catenin pathway, which is the only well-studied signaling system involved in the induction of EMT at present (Dudas and Kaartinen, 2005).

3.3.5.4 Signaling pathways in Epithelial-mesenchymal interactions

Recent studies have started to address how the coordinated reciprocal signaling interactions between the palatal epithelium and the underlying mesenchyme takes place during palatal shelf growth, elevation and fusion. These important findings first demonstrated that the bona fide TGF-β-BMP effector Msx1 is expressed in the palatal mesenchyme and controls a genetic hierarchy of bone morphogenetic proteins (BMPs) and sonic hedgehog (Shh) (Zhang et al., 2002). These investigators proposed that *Msx1*

expression induced by *BMP-4* in the anterior palate is also required to maintain levels of *BMP-4*. Moreover, *BMP-4* is required to induce *Shh* expression in the anterior palatal epithelium, which in turn signals back to the mesenchyme to induce cell proliferation and palatal growth. Because *Alk2/Wnt1-Cre* mutant mice display a defect in palatal shelf elevation (Dudas et al., 2004), it is believed that at least some of these mesenchymal BMP signals are mediated via ALK-2. Recently, it has been showed that Fgf10 (expressed in the mesenchyme) that signals via Fgfr2b (expressed in the epithelium) is also required in induction of epithelial expression of Shh and this network, in conjunction with the BMP signaling, is required both in the growth and in appropriate morphogenesis (shaping) of palatal shelves (Rice et al., 2004). Additionally, it was also reported that *TGF-β3*$^{-/-}$ mice display high levels of TGF-β1 in the palatal mesenchyme (Martinez-Alvarez et al., 2004), which was postulated to lead to aberrant epithelial expression of the zinc-finger transcriptional repressor Snail and a subsequent promotion of cell survival in the MEE. Therefore, mesenchymal TGF-β signaling is important in palatogenesis. This again can be supported by the fact that specific ALK-5 abrogation in neural crest cells could lead to severe facial cleft, including a cleft palate(Dudas and Kaartinen, 2005).

3.3.6 Prenatal palatal closure related to skeletal maturity of the jaws

The very early developmental stage in which the palatal shelves change direction from vertical to horizontal position has received the most interest (Andersen and Matthiessen, 1967; Burdi and Faist, 1967; Griffin, 1984; Luke, 1976; Sperber, 1981; Wood and Kraus, 1962). Kjaer's study (1989) has revealed an unknown maturity pattern of the skeletal structures at the time of palatal shelf elevating. The study showed that the skeletal maturation stage of the maxilla is apparently at the same time of palatal closure. However,

how the tissue in the palatal shelves interacts with the vomeral tissue components has not been elucidated. The study suggests that the timing of palatal shelf elevation is related to vomeral development because it consistently occurs prior to ossification of the paired vomer bones situated cranially to the shelves (Kjaer, 1989).

3.4 Cleft Palate

3.4.1 Introduction

The classification of cleft lip with or without cleft palate includes both isolated and syndromal forms and is the most common anomaly of human facial development (Cousley and Roberts-Harry, 2000). The distinct timing and exquisite coordination of developmental events leading to the formation of the primary palate and secondary palate clearly distinguish clefts of the primary palate (also called cleft lip) and clefts of the secondary palate (also called cleft palate) only as separate biological entities. However, it is recognized that there are many genetic pathways and cellular mechanisms in common (Mclnnes and Michaud, 2004).

Cleft palate affects approximately 1 out of 700 individuals with some variations in all ethnic groups all over the world (Dudas and Kaartinen, 2005). A cleft palate may result from disturbances at any stage of palate development: defective palatal shelf growth, delayed or failed shelf elevation, defective shelf fusion, failure of medial edge cell death, postfusion rupture and failure of mesenchymal consolidation and differentiation (Ferguson, 1987).

In mouse, the secondary palate is formed from outgrowths of maxillary processes of the first branchial arch at E12. The proliferation of the mostly neural crest-derived mesenchyme of palatal shelves leads to palatal shelf rapid growth, which then grow down

vertically along the sides of the tongue. At E14, the elongation of the lower jaw and other morphogenetic events direct rapid expansion of the oral cavity allowing descent of the tongue and subsequent elevation of the palatal shelves. Soon after the elevation, the palatal shelves start approaching each other and begin to fuse to form a single continuous palate. At this time the MEE becomes adherent (Taya et al., 1999). MEE cells then intercalate and form the palatal MES (Martinez-Alvarez et al., 2000b), and eventually disappear. Cleft palate can result from any failure in any of these steps.

3.4.2 *Hoxa2* gene

Hoxa2 belongs to one of the most 3' paralogous groups of the *Hox* gene family (Fig. 3). It has already been cloned from a variety of species and has been extensively analyzed at the molecular and functional levels (Barrow and Capecchi, 1999; Barrow et al., 2000; Davenne et al., 1999; Gavalas et al., 1997; Gendron-Maguire et al., 1993; Grammatopoulos et al., 2000; Hao et al., 1999; Kanzler et al., 1998; Mallo and Brandlin, 1997; Nazarali et al., 2000; Pasqualetti et al., 2000; Prince and Lumsden, 1994; Rijli et al., 1993; Tan et al., 1992). During development *Hoxa2* is expressed in several tissues, including the neural tube and the neural crest-derived mesenchyme of the branchial area. In the neural tube, *Hoxa2* is expressed throughout the rostro-caudal (R-C) length of the spinal cord, with a dynamic expression pattern along the dorso-ventral (D-V) axis, starting in the ventral mantle region at E 10.5 and moving progressively to more dorsal areas, to be mostly expressed by cells in the dorsal horn at E18.5 (Hao et al., 1999). In the E8 mouse hindbrain, *Hoxa2* shows a rostral limit of expression at the border between r1 and r2 (Gavalas et al., 1997; Krumlauf, 1993; Prince and Lumsden, 1994). In this area of the neural tube, *Hoxa2* expression is also restricted along the D-V axis, showing higher

expression in a longitudinal column along the alar plate (Davenne et al., 1999). In the neural crest, *Hoxa2* is expressed in subsets of premigratory and migratory crest cells populating the second and more caudal branchial arches (Mallo and Brandlin, 1997; Nonchev et al., 1996; Prince and Lumsden, 1994). Importantly, although *Hoxa2* transcripts are detected in r2, this gene is not expressed in the neural crest once these cells start to migrate from r2 into the first branchial arch (Prince and Lumsden, 1994).

In mouse, disruption of the *Hoxa2* gene mainly affects second branchial arch development. Second arch skeletal elements (stapes, styloid process, lesser horn of the hyoid bone) are transformed into first arch-specific skeletal elements (incus, malleus and tympanic ring), arranged in a mirror image disposition to their first arch counterparts (Barrow and Capecchi, 1999; Gendron-Maguire et al., 1993; Rijli et al., 1993). This arrangement suggests a common source of information located between the first and second branchial arch (Rijli et al., 1993; Mallo and Brandlin, 1997), with a different interpretation of this common signal in neural crest cells expressing *Hoxa2*.

Hoxa2 expression is directly regulated by the transcription factor Krox20 (Nonchev et al., 1996; Tumpel et al., 2002). In contrast, *Hoxa2* expression in neural crest cell of the second branchial arch is tightly controlled by a number of elements, one of which binds to *Ap-2* family members. Mutation or deletion of this site in the *Hoxa2* enhancer abrogates expression in cranial neural crest cells but not in the hindbrain. These findings clearly demonstrate that *Hoxa2* is independently regulated in rhombomeres and neural crest cells, thus providing a mechanism for how neural crest cells can respond to the environment through which they migrate independently from the neural tube (Trainor, 2003b). As the transposed neural crest cells can be reprogrammed, it appears that neural

crest cells receive distinct cues in the branchial arch environments through which they migrate to give rise to their proper regional identity. Furthermore, the importance of the size of the transposed cell community indicates that a far more complex balance of molecular and cellular interactions are involved in neural crest cell and branchial arch patterning than was previously believed (Trainor, 2003b).

3.4.3 *Hoxa2* gene and the secondary cleft palate (CLP)

It has been reported previously that *Hoxa2* mutants possess CLP at high penetrance (Gendron-Maguire et al., 1993; Rijli et al., 93; Barrow and Capecchi, 1999). A cleft in the secondary palate occurs with 82% penetrance in *Hoxa2* mutant mice (14/17) (Barrow and Capecchi, 1999), which is identical to the 82% reported by Rijli et al. (1993). The reason for this defect was not clear as *Hoxa2* is reported not to be expressed in neural crest cells of the first arch (Prince and Lumsden, 1994). Barrow and Capecchi (1999) reported that the *Hoxa2* mutants exhibit severe defects in the extrinsic tongue and hyoid musculature at 100% penetrance. The presence of defects within the extrinsic tongue and hyoid musculature was reported to be correlated perfectly with the presence of CLP: when the hyoglossus was prevented from attaching to the greater horn of the hyoid, CLP was observed. The hyoglossus muscle functions to depress the lateral edges of the tongue. It is possible that, during embryogenesis, this extrinsic tongue muscle plays a vital role in flattening the tongue such that the flanking palatal shelves can lift and fuse above it. However, without the function of this muscle, the tongue adopts a posture that blocks palate shelves closure (Barrow and Capecchi, 1999). Indeed, it has been demonstrated that, in rat development, myogenesis of the tongue muscles including the hyoglossus are functional prior to palatal shelf closure (Wragg et al., 1972). It is therefore plausible that

changes in the morphology of the tongue during embryonic development may play a role in normal palate formation (Barrow and Capecchi, 1999).

Histological analysis shows, prior to palatal shelf closure, there is no major difference in the morphology of the tongue between wild-type and *Hoxa2* mutant embryos. During palatal closure, the morphology of hyoglossus muscle is changing in wild-type embryos and accompanied by a flattening of the tongue. At the same time in mutants with a normal palate, similar changes in the morphology of the hyoglossus and in the flattening of the tongue are observed as in wild-type embryos. In mutants with a CLP, however, the tongue is not flattened and the lateral edges of the tongue are abnormally raised. It was observed that in *Hoxa2* mutant homozygotes, the ectopic trajectory of two muscles, the stylohyoideus and the styloglossus, prevents the attachment of the hyoglossus muscle to the greater horn of the hyoid (Barrow and Capecchi, 1999).

Barrow and Capecchi (1999) indicated the perfect correlation between the presence of CLP and the absence of attachment of the hyoglossus muscle to the greater horn of the hyoid bone suggests that the position of the tongue plays a critical role in normal palate formation. In the absence of a functioning hyoglossus muscle, the tongue is not properly positioned on the floor of the mouth and thus obstructs the lifting of the palatal shelves above the tongue, preventing the normal palatal shelf fusion resulting in a CLP. However, Ohnemus et al (2001) demonstrated that the hyoglossus was always inserted in the hyoid regardless of the presence or absence of a CLP.

3.4.4. Molecular pathogenesis of cleft palate (CLP) and signaling pathways

Mutations in many genes have been shown to cause cleft of the secondary palate in mice. Most of these mouse mutants have other multiple craniofacial abnormalities and the pathogenesis of the CLP has not been well studied.

Some of the molecular signaling pathways involved in the epithelial-mesenchymal interactions have recently been unraveled. TGFβr2 receptor is expressed both in the MEE cells and in the mesenchyme adjacent to MEE during secondary palate development. The CLP in the conditional *Tgfβr2* mutants was shown to be due to about 10% decrease in cell proliferation in the cranial neural crest derived mesenchymal cell population in the palatal shelves from E14.5. In these mutants the palatal fusion was not disturbed; when palatal shelves were placed in organ culture they fused. Thus, in these mutants the epithelial function of *TGF-β3* may not be fully blocked, and there may be a cell autonomous requirement for *TGF-β* signaling in the cranial neural crest derived palatal mesenchyme (Ito et al., 2003).

The *Tgfβr2* mutants showed 2.5 times elevated levels of *Msx1* expression in the palatal mesenchyme (Satokata and Maas, 1994). In *Msx1*$^{-/-}$ animals the mesenchymal proliferation in the anterior palatal shelves achieved by epithelial-mesenchymal interactions that combine Bmp and Shh signaling pathways is disrupted leading to CLP (Zhang et al., 2002). In these mice, the primordial palatal shelves formed and elevated normally but failed to contact each other and did not fuse (Zhang et al., 2002). When *Msx1*-deficient palatal shelves were placed in contact with each other in organ culture, the shelves fused indicating that this was not the cause of the CLP. The CLP phenotype was rescued by crossing the *Msx1*-deficient mice with transgenic mice that overexpressed

human *BMP4* under the control of the *Msx1* promoter. Furthermore, the researchers showed that palatal mesenchyme expresses Bmp4 and that ectopic Bmp4 protein subsequently induces expression of Shh in palatal epithelium. Ectopic Shh protein induces the expression of Bmp2 in the mesenchyme, thus indicating that Shh signals from the epithelium back to the mesenchyme. Bmp2 then acts as a mitogen to stimulate cell proliferation in the mesenchyme. A similar signaling network has been established previously in tooth development (Bei et al., 2000; chen et al., 1996; Dassule et al., 2000; Gritli-Linde et al., 2002). It is important to note that both Bmp2 and Bmp4 use the same receptors (BmprI and II in homo- and heterodimers) for their signaling. Interestingly, even though *Msx1, Bmp2, Bmp4* and *Shh* were found to be expressed only in the anterior region of the palatal shelves (anterior to first molar tooth) at E12.5 and E13.5, posterior regions were also affected (Zhang et al., 2002). It has also been reported that *Shh* is expressed along the entire anteroposterior axis of palatal epithelium at E13 (Keranen et al., 1999), and that mesenchymal Fgf10 regulates epithelial expression of Shh through the epithelial receptor Fgfr2b. It is possible that the expression of Shh is under complex regulation where Bmp signaling primarily regulates the anterior expression of Shh, and Fgf signaling along the whole anterior-posterior length of the MEE.

4. Outlines of present research

A whole mouse organ palatal culture model has previously been established in our laboratory. Penetrance of induced CLP was then determined in this *in vitro* culture system, without any interference from the tongue (Zhang, W., M.Sc. Thesis, 2003).

My basic experimental design was to develop a construct of a retroviral vector (pLEGFP) that comprises *Hoxa2* cDNA in a sense or antisense orientation. These retroviral vectors fused with *Hoxa2* (pLEGFP-*Hoxa2* sense or pLEGFP–*Hoxa2* antisense) were then transfected separately into an EcoPack2-293 packaging cell line to produce retroviral particles. As the recombinant retroviral vector integrates into the genome of EcoPack2-293 cell line containing the viral gene envelope, retroviral particles carrying *Hoxa2* gene in sense or antisense orientation are generated. Viral titers for the sense and antisense *Hoxa2* retroviral particles were then determined by transducing NIH 3T3 cells. Subsequent addition of the viral cell supernatant to the mouse palate organ culture media resulted in the infection of the palatal organ culture.

The effect of these retroviral particles on whole organ palatal culture was determined by measuring palate parameters, including Length of Palate Shelf (LPS), Length of Fused Portion (LFP), Frequency of Contacted Palates (± Fusion), Frequency of Fused Palates (FFP) and Ratio of Fused Portion to the Length of Palate Shelf (RFPPS). The *Hoxa2* gene expression in the wild-type organ palate culture and cultures treated with retroviral particles were measured by real-time RT-PCR. Hoxa2 protein was detected with western blot analyses.

5. Experimental Methods

5.1 Media preparation and palatal organ culture

The palatal organ culture medium is comprised of improved MEM Zinc Option (Richter's Modification) and F12 Nutrient Medium (GIBCO, Grand Island, NY) (1:1), formulated as described in (Abbott et al., 1999). The medium was supplemented with 1% fetal bovine serum, 6 mg/ml BSA, 10 μg/ml transferrin, 10 ng/ml selenium, 50 μg/ml sodium ascorbate, 2.4 mg/ml glucose, 0.6 mg/ml L-glutamine, 50 μg/ml streptomycin and 50 units/ml penicillin (Sigma Chemical, St. Louis, MO). Sterile 60 ml culture bottles (VWR International, West Chester, PA) containing 10 ml of palatal organ culture medium were flushed with a gas containing 50% O_2, 45% N_2 and 5% CO_2 for 2 minutes after the addition of up to 4 palatal explants. The bottles were then capped and placed in a 37°C incubator (Model 400, Robbins Scientific, Sunnyvale, CA), circulated at 12-15 revolutions per minute. Media and gases were changed and replenished daily.

5.2 Palate dissection

Mouse whole organ palates were dissected as described by (Abbott and Buckalew, 1992); Cuervo et al 2002. Time-pregnant CD-1 mice at embryonic day (E) 12.5 were used (vaginal plugs were detected at 0.5 d.p.c.). Mice were anaesthetized with halothane (MTC Pharmaceuticals, Cambridge, Ontario) and fetuses were aseptically removed from the uterus and placed in Hank's balanced solution (Sigma Chemical, St. Louis, MO). Secondary palates were dissected from the embryos by performing two parallel horizontal cuts with microdissecting scissors through the oral opening above the tongue, and at the level of the eyes (Fig. 5). If any excess mandible or tongue remained it was removed with the fine microdissecting scissors. A tissue forcep was used to gently place

palatal explants into each culture bottle. The culture bottles were revolved (12-15 rpm) inside a temperature-controlled incubator for 3 days (37°C). Two parameters, Length of Palate Shelf (LPS) and Length of Fused Portion (LFP) (Fig. 6), were measured with an electronic digital micrometer under a dissecting microscope (Model 312684-122, Bausch & Lomb, Rochester, NY). Determination of whether the palatal shelves were simply contacted or completely fused was made by gently performing a separation of the shelves with a pair of forceps, and observing whether or not the two palatal shelves could be pulled apart. Frequency of Contacted Palates (±Fusion) and Frequency of Fused Palates (FFP) were then assessed, and a Ratio of Fused Portion to the length of Palatal Shelf (RFPPS) was calculated.

5.3 *Hoxa2* cDNA digested from the recombinant plasmid pRSV-*Hoxa2*

Hoxa2 cDNA was digested from the recombinant plasmid pRSV-*Hoxa2* with *Hind* III and *Xho* I (Nazarali et al., 1992; Tan et al., 1992). The reactions included 0.4-0.8 μg of plasmid pRSV-*Hoxa2*, 2 μl of *Hind* III (Invitrogen, Carlsbad, CA) and 2 μl of *Xho* I (Invitrogen, Carlsbad, CA) and 3 μl of 10 × Reaction Buffer 2 (Invitrogen, Carlsbad, CA) to give a final reaction volume of 30 μl in water which was incubated at 37 °C. After 1 hour of incubation, 2 μg of RNase A (Sigma, St. Louis, MO) was added to the reaction mixture to digest contaminating RNA. DNA fragments were separated by gel electrophoresis. The *Hoxa2* band (about 1200 kb) was cut from the gel and purified with Montge DNA Extraction Kit (Millipore, Billerica, MA) according to the manufacturer's standard protocol.

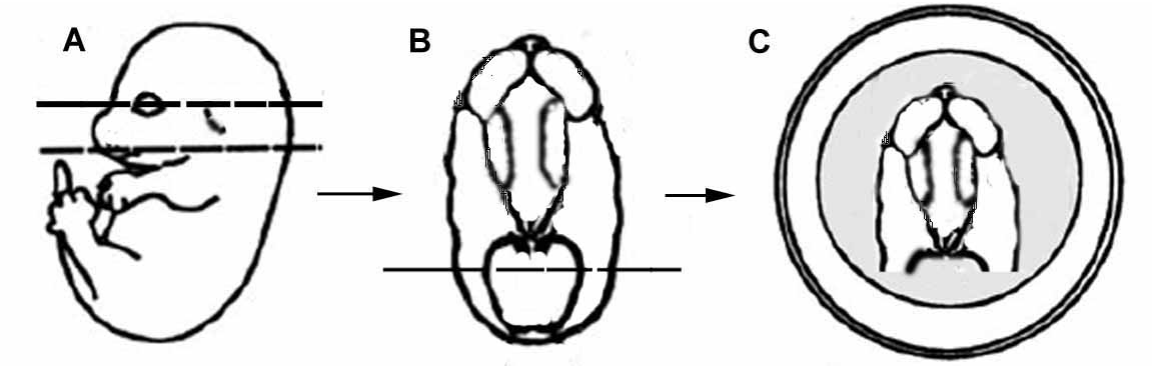

Figure 5 Schematic diagram of palatal dissection used in this study. **(A)** Mouse secondary palates were dissected from embryos by performing two transverse cuts, one just through the eye, and the second through the mouth above the tongue to maintain an intact nasal cavity. **(B)** From this slice in (A) two thirds of the spinal cord was removed as indicated. **(C)** Dissected palates were placed inside the bottle containing the growth medium (Redrawn from Cuervo et al., 2002).

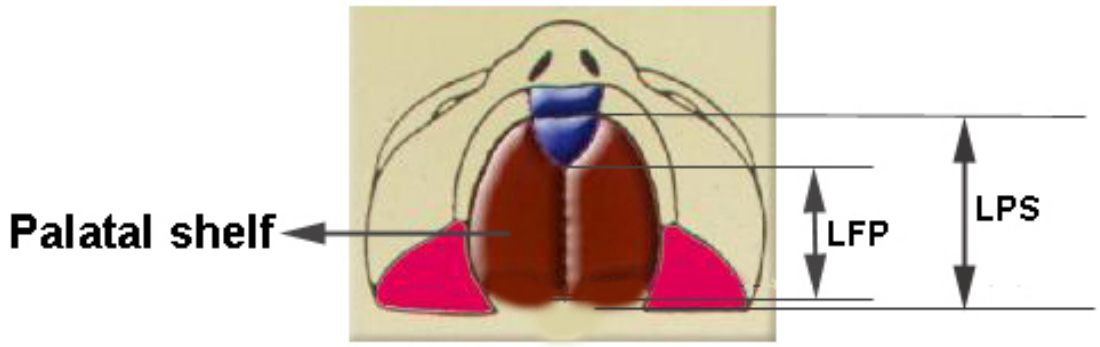

Figure 6 A schematic diagram of a secondary palate showing parameters measured on palatal shelves. LFP: Length of Fused Portion. LPS: Length of Palatal Shelf.

5. 4 *Hoxa2*-sense and antisense constructs

Hoxa2 antisense construct was developed by cloning the *Hoxa2* cDNA into the retroviral vector pLEGFP-C1 (BD Biosciences, Clontech, Mountain View, CA) at *Hind* III and *Xho* I restriction sites. *Hoxa2* sense was developed by addition of reverse restriction enzyme sites of *Hind* III and *Xho* I with PCR (PTC-100, Perking Elmer, Boston, MA) followed by subcloning into the retroviral vector pLEGFP-C1. The following primers were used for PCR: sense 5'-ggctcgagccatgaattacgaatttgagcg-3', antisense 5'-ggaagcttttagtaattcagatgctgtaggtcg-3'. PCR conditions used were; denaturation at 94 °C for 70 sec, annealing at 54 °C for 70 sec, followed by extension at 72 °C for 2 min. A total of 35 PCR cycles were used in the amplification process. The pLEGFP-*Hoxa2* sense and antisense constructs were sequenced with an ABI PRISM^{TM} system (carried out at PBI, National Research Council Canada at the University of Saskatchewan) (See Appendix). All recombinant plasmids were purified with EndoFree Plasmid Maxi Kit (Qiagen, Mississauga, Ontario).

5.5 Culturing EcoPack2-293 packaging cell line

The EcoPack2-293 packaging cell line (BD Biosciences, Clontech, Mountain View, CA) was cultured on collagen-coated plates at 37 °C with 5% CO_2. To make collagen stock solution, 15 ml of 0.1% acetic acid solution was aseptically added to a 100 mg bottle of collagen – type 1 (Sigma, St. Louis, MO). After stirring at RT for 2-5 hours, collagen solution was transferred to a 100 ml round bottom bottle and an additional 18.3 ml of 0.1% acetic acid was added. The stock solution was stirred vigorously overnight. Collagen stock solution (300 µl) was placed aseptically on each 100 mm tissue culture dish (Corning, Acton, MA) and the solution was spread evenly over the surface of the

dish using a sterile glass pipette. The coated culture dishes were then rinsed with 2 × 2 ml of growth medium (see below) and left to air dry inside the laminar flow hood with a partially covered lid for 24 hours. The packaging cells were maintained in Dulbecco's Modified Eagle's growth Medium (DMEM) containing 584 μg/ml L-glutamine and 4.50 mg/ml glucose supplemented with 10% (v/v) fetal bovine serum (FBS) (HyClone, Logan, UT), 3.70 mg/ml of sodium bicarbonate, 1 mM sodium pyruvate and 1% (v/v) antibiotic-antimycotic (Sigma, St. Louis, MO). The cells were plated at a density of 10^6 cells per 100 mm dish and split every 2-3 days upon reaching 80-90% confluency. The cells were washed with Dulbecco's Phosphate Buffered Saline (DPBS) containing 0.2 mg/ml of KCl, 0.2 mg/ml of KH_2PO_4, 8 mg/ml of NaCl and 1.14 mg/ml of Na_2HPO_4 (Sigma, St. Louis, MO) and trypsinised with 0.5% trypsin/0.02% EDTA (Sigma, St. Louis, MO). After a stable cell culture was established, cells were suspended in a cell freezing medium containing 70% FBS and 10% DMSO at 1-2 × 10^6 cells/ml in 1.5-ml sterile cryogenic vials (Nalge Nunc International, Rochester, NY). The vials were placed in a cell freezing container (Nalge Nunc International, Rochester, NY) at -80 °C overnight and then stored under liquid nitrogen.

5.6 Product of replication-incompetent retrovirus

*Hoxa*2 sense or antisense cDNA was cloned into the pLEGFP retroviral vector (see Section 5.4). The transcript of the enhanced green fluorescent protein (*EGFP*) gene fused to *Hoxa*2 sense or antisense cDNA is under the control of a human cytomegalovirus (CMV) immediate early promoter (P_{CMV}). A neomycin resistance (Neo') gene encoding for neomycin phosphotransferase, is under the control of the promoter in LTR for antibiotic (G418) selection in eukaryotic cells. Recombinant retroviruses, bearing the

EGFP reporter gene, were generated from a stable transfection system using a SuperFect Transfection Reagent (Qiagen, Mississauga, Ontario) with the following three plasmids: pLEGFP, pLEGFP-*Hoxa2* sense and pLEGFP-*Hoxa2* antisense. The EcoPack2-293 packaging cell line was plated at a density of 1.5-2.0 × 10^6 cells in 5 ml of complete growth medium in a 60 mm dish and the cells allowed to reach 80-90% confluency on the day of transfection. An aliquot of 5 µg DNA (pLEGFP: 0.14 µg/µl; pLEGFP-*Hoxa2* sense: 0.25 µg/µl; pLEGFP-*Hoxa2* antisense: 0.14 µg/µl) dissolved in TE buffer (pH 8.0) was diluted with the cell growth medium (without FBS or antibiotic) to a total volume of 150 µl. SuperFect Transfection Reagent (30 µl) was add to the DNA solution, vortexed for 10 sec and incubated for 5-10 min at RT to allow transfection-complex formation. Cell growth medium (1 ml) was then added to the reaction tube, and mixed by gently pipetting up and down twice, then transferred immediately to the cells in the 60 mm dish. After incubation for 2-3 h at 37 °C in 5% CO_2, 3-4 ml of growth medium was added to the transfected cells, and incubated for a further12-15 h, before changing to fresh growth medium. Transfection efficiency was verified by EGFP protein expression 48 h post-transfection with the Reflected Light Fluorescence Microscope (BX-FLA, OLYMPUS, Japan). The transfected cells were split and cultured for an additional 2-3 days to reach 80% confluency for a stable colony selection (Fig. 7).

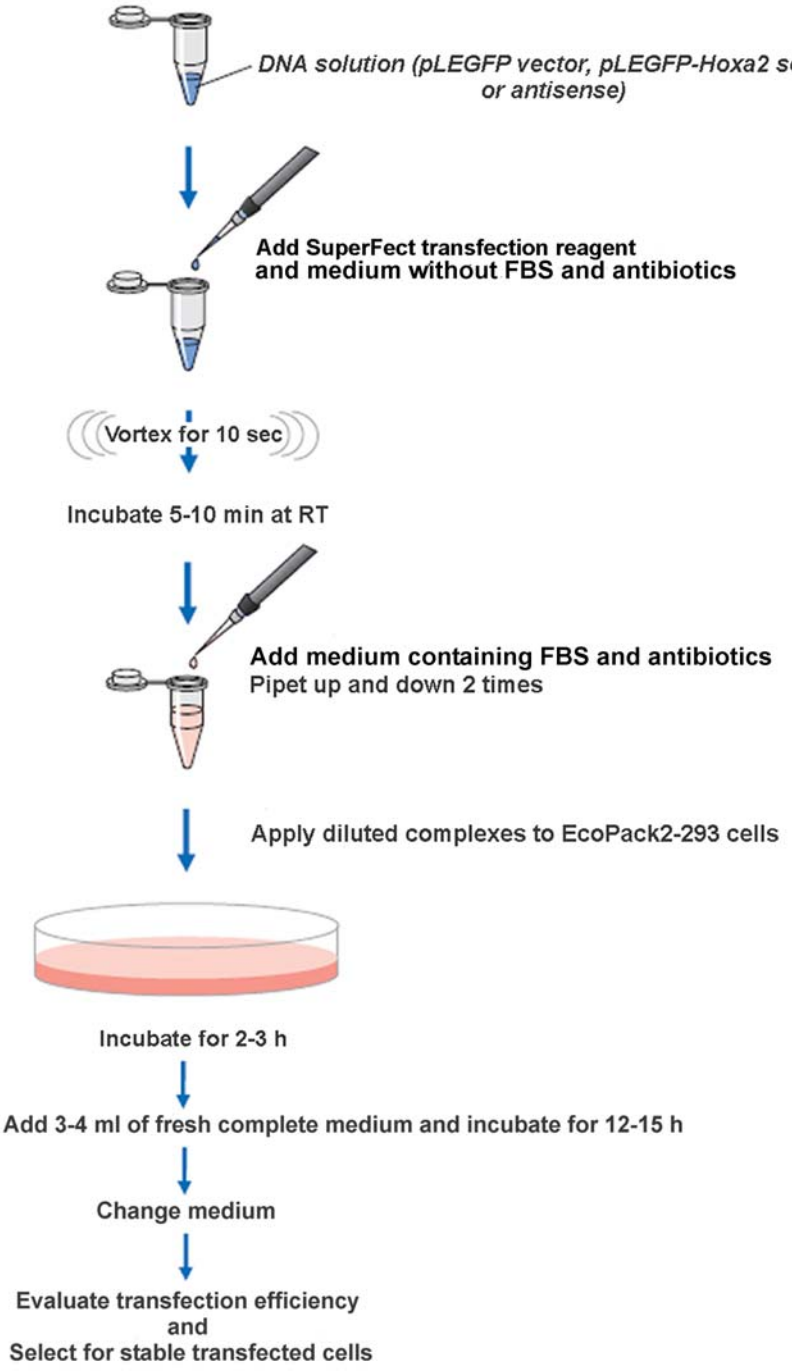

Figure 7 Transfection Procedures for EcoPack 2-293 cells

5.7 Titration of antibiotic stocks (kill curves)

Prior to using G418 to establish a stable cell line, it was necessary to titrate G418 to determine the optimal concentration required for selection with the EcoPack2-293 packaging cell line and NIH 3T3 cells. Two experiments were performed for this titration: To determine the optimal drug concentration, 2×10^5 cells were plated in each of six 10 mm plates containing 10 ml of the appropriate complete medium (see Section 5.5 and 5.10) with varying amounts of G418 (Sigma, St. Louis, MO) (at 0 μg/ml, 50 μg/ml, 100 μg/ml, 200 μg/ml, 400 μg/ml and 800 μg/ml), respectively. The cells were incubated for 10-14 days and the selection medium was replaced every four days. The optimal drug concentration of 400 μg/ml for EcoPack2-293 cell line and of 700 μg/ml for NIH 3T3 cell were determined, which were the lowest drug concentration that began to produce a massive cell death in 5 days, and killed all the cells within two weeks. To determine the optimal plating density, the cells (EcoPack2-293 or NIH 3T3) were plated at several different densities (5×10^6, 1×10^6, 5×10^5, 2×10^5, 1×10^5 and 5×10^4 cells on each 10 mm dish in the appropriate growth medium, with 400 μg/ml G418 for EcoPack2-293 cell line and 700 μg/ml G418 for NIH 3T3 cells), and incubated for 5-14 days, replacing the selection medium every four days. The optimal plating density of each cell type was determined with a plating density that allowed the cells to reach ~80% confluency before massive cell death began at day 5, which was 1×10^6 cells for the EcoPack2-293 cell line and 2×10^5 for NIH 3T3 cells.

5.8 Selecting a stable retrovirus-producing cell line

The transfected packaging cells were plated at 1×10^6 cells/100 mm plate in growth medium containing 400 μg/ml of G418 2-3 days post-transfection and the selection

medium was replaced every 3 days. After 8-10 days the colonies were visible and large, healthy colonies were isolated using sterile cloning cylinders (SCIENCEWARE, VWR International, West Chester, PA) and sterile silicon grease (Dow Corning, VWR International, West Chester, PA). About 50 colonies of each type of retrovirus-producing cell line were screened and transferred to a 24-well plate.

5.9 Generation of high titer retroviral stocks

The isolated colony cells were maintained on 24-well plates in the medium (see Section 5.5) supplemented with 10% BCS (HyClone, Logan, UT) until they were 50%-90% confluent. The medium was replaced by one-half volume and incubated for 1-3 days. The yellow supernatant containing the retroviral particles were harvested, and the samples centrifuged at 1535 rpm for 10 min at 4 °C (Eppendorf 5403 Centrifuge, Hamburg, Germany) to remove cellular debris. After filtering through a 0.45 μm filter (SARSTEDT, Nümbrecht, Germany) the retroviral particles were titered immediately (see below, Section 5.10). About 10-well-colony cells were screened to titer for each type of retroviral producer cells. Once the producer cell line with the highest titer was identified, these cells were split and grown on 10 mm plates or 75-flasks (Corning, Acton, MA) for a large-scale collection of retrovirus stocks. The supernatant was collected as described above and stored at -70°C. The best retroviral producer cells were continued to passage until they could be frozen. These producer cells were stored in liquid nitrogen in a freezing medium containing 10-15% DMSO.

5.10 Infection of NIH 3T3 cells to determine viral titers

The day before infection, NIH-3T3 cells were plated at 8×10^4 per well in 6-well plates with 2 ml of DMEM supplemented with 10% BCS, 1% Ab/Am at 37° C, 5% CO_2

and 100% relative humidity. On infection day, a total of 10 ml of complete medium with 6 μg/ml of sterile polybrene (Sigma, St. Louis, MO) in 0.9% NaCl solution was prepared. Six 10-fold serial dilutions were prepared as follows: 1.35 ml of medium prepared as above was added to each of six 1.5 ml microcentrifuge tubes. Filtered supernatant (150 μl) containing retroviral particles was added to tube 1 and mixed well. An aliquot of 150 μl of viral stock solution was then transfered from tube 1 to tube 2, and mixed by inverting. This series of 10-fold dilution was continued from tube 2 to 6. NIH 3T3 cells were infected by adding 1 ml of solution from each tube to each of the 6 wells. The infected cells were left for a further 24-30 h to allow transgene expression and the medium was replaced with a selection medium containing G418 (700μg/ml). The selection medium was changed every third day, for a period of 21 days. Once the non-resistant cells died and resistant colonies were visible, the medium was removed. The six-well plate was dried and the colonies were counted. The titer was then calculated from the number of colonies present at the highest dilution, multiplied by the dilution factor (see below). The titer was determined for each retroviral sample and the process was repeated three times. The average was taken based on the three independent results. In the presence of polybrene, titers of 1.8×10^7 cfu/ml, 6.7×10^6 cfu/ml and 4.0×10^6 cfu/ml were established for control pLEGFP, pLEGFP-*Hoxa2* sense and pLEGFP-*Hoxa2* antisense retroviral particles, respectively.

For example: If 3 colonies were presented in the 10^6 dilution, the titer would be:

3 colony forming units (cfu) × 10^6 = 3 × 10^6 cfu/ml

5.11 Infection of palatal organ culture

The palatal organ cultures were infected with retroviral particles in the presence of 6 μg/ml of polybrene at E12.5 and at E13.5. Various quantities of viral stocks were added to the palatal organ culture medium to reach serial titers of 10^5, 10^4 and 10^3cfu/ml, respectively. The palates were assessed after 3 days and measured by the same parameters used for the wild-type palatal cultures (see Section 5.2). The desired transduction effect was verified by observing EGFP expression using a confocal microscope (Zeiss LSM 410 invert, Zeiss, Ontario).

5.12 Total RNA isolation

The palatal shelves were removed under a dissecting microscope, and immediately frozen in liquid N_2. Palatal shelves from wild-type mouse embryos at E12.5, E13.5, E14.5 and E15.5 were designated as wild-type groups, while palatal shelves treated with pLEGFP, pLEGFP-*Hoxa2* sense or antisense retroviruses were designated as sample groups. Total RNA was prepared from a pair of palatal shelves by extraction with TRI® Reagent (Sigma, St. Louis, MO). Tissues were placed in 1.5 ml microcentrifuge tubes with 250 μl of TRI® Reagent and homogenized. The homogenates were then stored for 15 minutes at RT, and extracted with 150 μl of 1-bromo-3-chloropropane (BCP) (Sigma, St. Louis, MO). The aqueous phase was combined with an equal volume (150μl) of isopropanol (EMD, Gibbstown, NJ) to precipitate total RNA. The precipitate was centrifuged to form a pellet, subsequently washed with 75% ethanol and air-dried. The isolated total RNA was then re-dissolved in DEPC-treated water (Sigma, St. Louis, MO). Total RNA concentration was determined at OD_{260} using an Ultraspec 3100 *pro* Spectrophotometer (Biochrom Ltd. Cambridge, England).

5.13 Real-time RT-PCR

Before RT-PCR reaction was performed, total mRNA solutions were diluted to a concentration of 50 ng/µl, and 1.6 µl and 2.0 µl of which were taken for reverse transcription reaction for wild-type and virus treated samples, respectively. Omniscript® or Sensiscript® RT kit (Qiagen, Mississauga, Ontario) and random hexamers (Invitrogen, Carlsbad, CA) were used for RT-PCR reaction. Real-time PCR with TaqMan primers (Applied Biosystems, Foster City, CA) was used to quantify *Hoxa2* mRNA. The amplification was performed in a Cepheid Smart Cycler® System (Roche Molecular System, Inc., Alameda, CA). Three microliters of the RT-PCR reaction was amplified in a 20 µl PCR mixture, containing 1 × Universal PCR master mix (Applied Biosystems, Foster City, CA) and 900 nM of PCR primers and probes designed by Applied Biosystems. The transcript of the *Beta-actin* housekeeping gene was amplified as an endogenous control of RNA quality. Four samples were analyzed at each embryonic stage. The real-time PCR conditions were 50°C/2 min (for optimal AmpErase uracil-N-glycosylase [UNG] activity), 95°C/12 min followed by 95°C/15 sec and 60°C/1 min for 45 cycles. The Smart Cycler® System established the threshold cycle (C_T) values needed to reveal the minimal amount of amplified material of the target transcript. The values of the total *Hoxa2* and *Beta-actin* transcript at each embryonic stage were calculated with the averaged C_T values of each sample, and extrapolated from standard curves. The normalized value of *Hoxa2* was established by dividing the average *Hoxa2* value with the average *Beta-actin* value at each embryonic stage, and this normalized *Hoxa2* value was then standardized to a relative E15.5 *Hoxa2* value in wild-type groups.

5.14 Western blot analysis

Palatal shelves were removed from timed-pregnant mice and extracted with 10 µl of 1% SDS and 5µl of 2X loading buffer. The protein samples were then denatured at 90 °C for 10 minutes. A 12% SDS-PAGE gel were used to separate proteins according to the manufacturer's protocol (Invitrogen, Carlsbad, CA) and 7 µl of supernatant was loaded onto the gel. The protein was transferred and immobilized onto a PVDF transfer membrane (PolyScreen, PerkinElmer, Boston, MA) by using Xcell II Blot Module (Invitrogen, Carlsbad, CA) for wet transfer in 1 X transfer buffer containing 12 mM Tris, 96 mM glycine and 20% methanol, for 2 hrs at 30V/200 mAmp. Blocking of the membrane was carried out in 3% skim milk (PBS) at 4 °C for overnight. For detection of the Hoxa2 protein, the membrane was incubated for 2 hrs at room temperature with the rabbit anti-Hoxa2 antiserum (B579, generated in our lab) (Hao et al 1999; Nazarali et al 2000) at a dilution of 1:2000 in 3% skim milk/PBS. The membrane was then washed 3 X 20 minutes with PBS/0.8% Tween-20 (Sigma, St. Louis, MO) and incubated for 1 h at RT with the horse radish peroxidase (HRP) conjugated secondary goat anti-rabbit IgG (Bio-Rad, Hercules, CA), diluted 1:3000 in 3% skim milk /PBS. After visualization of Hoxa2 protein, the membrane was blocked in 3% skim milk (PBS) at 4 for overnight again for detection of actin protein. A 1:200 dilution of the mouse anti-actin (JLA20 monoclonal antibody, Developmental Studies Hybridoma Bank, Iowa City, IA) in 3% skim milk/PBS was used as the primary antibody. The membrane was incubated for 1 hr at room temperature. After it was washed for 3 X 20 minutes with PBS/0.8% Tween-20, a 1:3000 dilution of HRP conjugated goat anti-mouse IgM (Bio-Rad, Hercules, CA) was used as the secondary antibody and the membrane was washed 3 X 20 minutes in

PBS/0.08% Tween-20. Visualization of proteins was performed by a Western Lightening Kit (PerkingElmer Life Sciences, Inc., Boston, MA) as per manufacture's instructions, followed by exposure of the membrane to Kodak Scientific Imaging Film (X-OMAT Blue XB-1, Kodak, Rochester, NY) for 3 -10 sec.

5.15 Histological analysis

The wild-type and mutant mouse palatal tissue specimens were fixed in Bouin's and embedded in paraffin for histological analysis. Tissue sections (4-μm thick) were stained with Hematoxylin and Eosin at the Department of Pathology, Western College of Veterinary Medicine at the University of Saskatchewan.

5.16 Statistical analysis

For the purpose of statistical analysis, SPSS software was used. One-way Anova followed by the least significant difference (LSD)'s post hoc analysis was used for comparing the mean values between the control and virus treatment groups to determine where statistical differences had occurred ($p \leq 0.05$).

6. Results

6.1 A stage-dependent expression level of *Hoxa2* mRNA in developing palates

Real-time RT-PCR was used to quantify *Hoxa2* mRNA levels in wild-type mouse palates at developmental stages E12.5 to E15.5. Results from the quantitative analysis of murine *Hoxa2* gene in developing palates are presented in Table 1 and Table 2. Results show *Hoxa2* gene expression is detectable in the developing shelves from E12.5 through E15.5 (Fig. 8). Moreover, *Hoxa2* mRNA expression in the palate undergoes a quantitative decline in level from E12.5 to E15.5. The temporal pattern of the relative expression level of *Hoxa2* in the palatal shelves is in agreement with a decrease in Hoxa2 protein as detected by a previous immunohistochemical analysis performed in our laboratory (Zhang, W., M.Sc. Thesis, 2003).

Table 1 *Hoxa2* mRNA values in wild-type palatal shelves by real-time RT-PCR (N=4, date normalized to *β-actin* mRNA)

Embryonic stage (E)	Total *Hoxa2* mRNA (ng)	Total *β-actin* mRNA (ng)	*Hoxa2* Norm. to *β-actin*
E12.5	5.00 ± 0.659	10.25 ± 0.582	0.49 ± 0.070**
E13.5	3.35 ± 0.088	15.09 ± 0.506	0.22 ± 0.009
E14.5	2.80 ± 0.410	14.07 ± 0.857	0.20 ± 0.032
E15.5	2.69 ± 0.606	15.45 ± 0.821	0.17 ± 0.040

Results represent Mean ± SD
(**, $p<0.01$ compared with E13.5, E14.5 and E15.5, respectively)

Table 2 *Hoxa2* mRNA values in wild-type palatal shelves normalized to total RNA (N=4)

Embryonic stage (E)	*Hoxa2* mRNA (ng)	Total RNA (ng)	*Hoxa2* Norm. to Total RNA
E12.5	5.00 ± 0.659	80	0.063 ± 0.008*
E13.5	3.35 ± 0.088	80	0.042 ± 0.001
E14.5	2.80 ± 0.410	80	0.035 ± 0.005
E15.5	2.69 ± 0.606	80	0.034 ± 0.007

Results represent Mean ± SD. Total RNA indicated is the amount of RNA used before real-time RT-PCR. (*, $p<0.05$ compared with E13.5, E14.5 and E15.5, respectively)

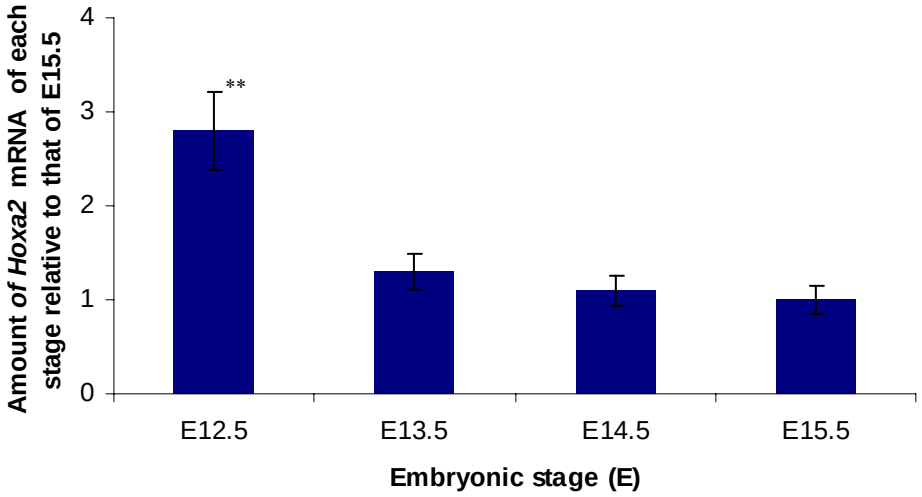

Figure 8 Detection of *Hoxa2* mRNA in mouse palatal shelves by real-time RT-PCR. Expression levels of *Hoxa2* mRNA at E12.5, E13.5, E14.5 and E15.5 relative to E15.5 in wild-type mouse embryos (data in Table 1). Bar chart represents Mean ± SD.

(**, $p<0.01$ compared to E13.5, E14.5 and E15.5, respectively)

6.2 Effects of retroviral (sense & antisense *Hoxa2*) infection on levels of *Hoxa2* gene expression in cultured palates

The wild-type mouse palatal organ cultures were transduced separately using a retrovirus expressing *Hoxa2* gene in sense and antisense orientation or control retroviral particles. Infection of palate organ cultures with *Hoxa2* sense retroviral particles induced *Hoxa2* overexpression, while infection with *Hoxa2* antisense retroviral particles inhibited *Hoxa2* expression.

To quantify the presence of *Hoxa2* expression in palates and determine the transduced efficiency of *Hoxa2* sense and antisense virus in palates, real-time RT-PCR was employed on control untreated and virus treated palatal shelves. An increase of *Hoxa2* mRNA was observed in palates treated with *Hoxa2* sense virus, while there was a decrease of *Hoxa2* mRNA in palates treated with the *Hoxa2* antisense virus (Tables 3 & 4). A comparison of this change in *Hoxa2* transcription by real-time RT-PCR in palates treated with *Hoxa2* sense and antisense virus and wild-type palates from E13.5 is shown in Tables 3 & 4. Confocal microscopy was used to demonstrate palatal shelves expressing EGFP from transduced retroviral particles carrying *Hoxa2* antisense (Fig. 9).

Table 3 *Hoxa2* mRNA values in retrovirus treated palatal shelves by real-time RT –PCR (N=4, data normalized to *β-actin* mRNA)

Palatal shelves treated with retrovirus	Total *Hoxa2* mRNA (ng)	Total *β-actin* mRNA (ng)	*Hoxa2* Norm. to *β-actin*
pLEGFP control retrovirus	3.97 ± 0.264	14.51 ± 0.572	0.274 ± 0.021
pLEGFP-*Hoxa2* sense retrovirus	7.78 ± 0.295	6.78 ± 0.295	1.148 ± 0.066**
pLEGPF-*Hoxa2* antisense retrovirus	1.47 ± 0.201	9.07 ± 0.411	0.162 ± 0.023*

Results represent Mean ± SD.
(**, $p<0.01$ compared with control and antisense retrovirus, *, $p<0.05$ compared with control retrovirus)

Table 4 *Hoxa2* mRNA values in retrovirus treated palatal shelves by real-time RT-PCR (N=4, data normalized to total RNA)

Palatal shelves treated with retrovirus	*Hoxa2* mRNA (ng)	Total RNA (ng)	*Hoxa2* Norm. to Total RNA
pLEGFP control retrovirus	3.97 ± 0.264	100	0.040 ± 0.003
pLEGFP-*Hoxa2* sense retrovirus	7.78 ± 0.295	100	0.078 ± 0.003**
pLEGPF-*Hoxa2* antisense retrovirus	1.47 ± 0.201	100	0.015 ± 0.002*

Results represent Mean ± SD. Total RNA indicated is the amount of RNA used before real-time RT-PCR. (**, $p<0.01$ compared with control and antisense retrovirus, *, $p<0.05$ compared with control retrovirus.)

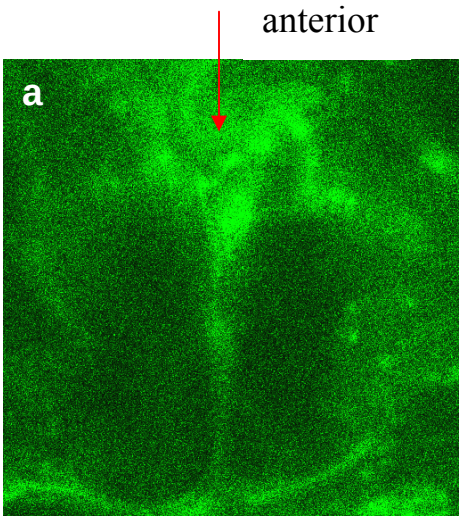

Figure 9 Retroviral expression and detection of EGFP protein in palatal organ culture using a confocal microscope. (a) A palatal organ culture treated with 10^{7} cfu/ml of retrovirus expressing EGFP. After 48 h of incubation, green fluorescence can be observed in midline epithelium under a confocal microscope (red arrow).

6.3 Impact of Hoxa2 protein expression in palatal shelves treated with *Hoxa2* sense and antisense retrovirus

Western blot analysis was performed to determine whether immunoreactive Hoxa2 protein in palatal shelves of control and retrovirus-treated organ cultures could be detected. This procedure employed a rabbit anti-Hoxa2 polyclonal antibody and a mouse anti-actin antibody as an internal control. A single Hoxa2 protein band was detected at approximately 42 kDa in all palatal shelves from E13.5 wild-type mice, and in palatal shelves treated with the control retrovirus, *Hoxa2* sense and *Hoxa2* antisense retrovirus. Actin protein band was also detected in all same samples at approximately 32 kDa, shown in Fig. 10. The results demonstrate no appreciable difference in Hoxa2 protein expression between palatal shelves from E13.5 wild-type mice and palatal shelves treated with the control retrovirus. However, Hoxa2 protein expression was appreciably decreased after treatment with *Hoxa2* antisense (Fig. 10 lane 3) and appreciably increased by treatment with *Hoxa2* sense (Fig. 10 lane 4) compared to Hoxa2 in palatal shelves from E13.5 wild-type mice and palatal shelves treated with the control retrovirus. These observations are consistent with prior results documenting *Hoxa2* expression in palatal shelves from E12.5 to E15.5 by real-time RT-PCR (Fig. 8). The change of Hoxa2 protein expression after treatment with *Hoxa2* sense and antisense is also consistent with real-time RT-PCR results of the same treatment samples (Tables 3 & 4). The western blot analysis provides additional support for the presence of Hoxa2 protein in palatal shelves.

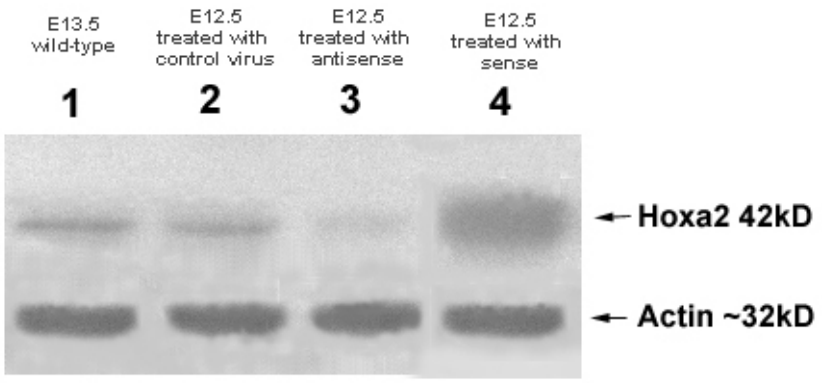

Figure 10 Western blot analysis of Hoxa2 proteins extracted from mouse palatal shelves. A single Hoxa2 band is observed at 42 kD and control actin protein band at ~ 32 kD. Lane 1: a pair of palatal shelves from E13.5 wild-type mouse; Lane 2: a pair of palatal shelves from E12.5 treated with control retrovirus for 24 hrs; Lane 3: a pair of palatal shelves from E12.5 treated with *Hoxa2* antisense retrovirus for 24 hrs; Lane 4: a pair of palatal shelves from E12.5 treated with *Hoxa2* sense retrovirus for 24 hrs.

6.4 Effect on palate development and fusion after infection with *Hoxa2* sense and antisense retrovirus

The wild-type mouse palatal organ cultures were infected separately using a retrovirus expressing *Hoxa2* gene in sense and antisense orientation or control retroviral particles. The impact of the effect of the retroviral treatment on the palates is summarized in Tables 5-7 and Figures 11-13**.** The palatal shelves for most titers in sense and antisense virus treated groups appear to be relatively smaller in length than the ones measured in the control group (Fig.11). In the sense group (Fig. 12), the absolute length of the fused portion was increased in the 0.8×10^5 cfu/ml titer group and decreased at lower titers ($1.6 \times 10^3 - 4.0 \times 10^3$ cfu/ml) compared with control virus treated group. However, only the absolute length of fused portion in 1.6×10^3 cfu/ml and 0.8×10^5 cfu/ml viral treated groups showed statistical significance. A similar increase and a more significant trend were also observed in the group treated with the antisense virus (Fig.12). It appears however, that this increased length of palatal fusion is more sensitive to *Hoxa2* antisense, since this trend appeared to start at a much lower retroviral titer (0.08×10^5 cfu/ml). Interestingly, in palates treated with antisense viruses, the length of the fused portion increased significantly in 0.8×10^5 cfu/ml titer (Fig.12), and with increasing titers the length of the fused portion appeared to increase relative to the length of the palatal shelves (compared with the control group). Therefore, the ratio of the length of the fused portion to the length of palatal shelves observed in the antisense group appears to be relatively large compared to the control group from that titer (Fig. 13). These observations suggest that *Hoxa2* may play a role in regulating the MEE cells proliferation

from E14 to E15. Furthermore, this gene could be involved in a signaling mechanism during palate fusion.

In addition, the frequency of contacted palates (± fusion) and frequency of the fused palates (FFP) were also determined. The values are summarized in Table 8 and Figure 14. While control pLEGFP retrovirus did not cause detectable effects compared with the wild-type group (See Table in Appendix), the *Hoxa2* sense and antisense retrovirus did have a significant negative effect on palate fusion (Table 8 and Fig.14). Palates transduced with the lowest titer of *Hoxa2* sense, results in a fusion rate of 72.7%, which is somewhat close to that of the palates treated with the control virus. However, in palates transduced with higher sense titers (2.4×10^5 or 3.2×10^5), we observed a fusion rate in the range of 41.2% and 50.0% respectively. The antisense group also shows similar defects in fusion to that of the sense group. Although results suggest a more profound effect in palate fusion with the antisense virus, compared with that at the frequency of lowest sense retrovirus or control virus titer. At the low antisense titers fusion rates are comparable with a fusion rate observed in palate organ cultures from *Hoxa2*-/- mutant mice (44.4%) (Zhang, W., M.Sc. Thesis, 2003).

Table 5 Effects of control retrovirus treatment on cultured mouse palates

	Titer (cfu/ml)	0.016×10^5 (n=22-24)	0.08×10^5 (n=19-22)	0.4×10^5 (n=16-22)	0.8×10^5 (n=18-22)	1.6×10^5 (n=20-21)	2.4×10^5 (n=17-21)	3.2×10^5 (n=16-21)
Control Retrovirus	**Length of palatal shelf (mm)**	1.354±0.166	1.333±0.075	1.298±0.051	1.395±0.090	1.384±0.056	1.412±0.129	1.329±0.118
	Length of fused portion (mm)	0.768±0.274	0.616±0.079	0.608±0.145	0.613±0.102	0.683±0.011	0.630±0.317	0.670±0.216
	Ratio of length of fused portion to length of palatal shelf	0.565±0.161	0.467±0.052	0.465±0.169	0.439±0.038	0.549±0.073	0.505±0.121	0.496±0.110

Results represent Mean ± SD.

Table 6 Effects of *Hoxa2* sense retrovirus treatment on cultured mouse palates

	Titer (cfu/ml)	0.016×10^5 (n=22-24)	0.08×10^5 (n=19-22)	0.4×10^5 (n=16-22)	0.8×10^5 (n=18-22)	1.6×10^5 (n=20-21)	2.4×10^5 (n=17-21)	3.2×10^5 (n=16-21)
***Hoxa2* Sense Retrovirus**	**Length of palatal shelf (mm)**	1.273±0.248	1.182±0.066**	1.242±0.056**	1.326±0.045*	1.288±0.105**	1.278±0.107**	1.306±0.097
	Length of fused portion (mm)	0.554±0.164*	0.572±0.091	0.566±0.146	0.708±0.148*	0.735±0.278	0.624±0.239	0.751±0.109
	Ratio of length of fused portion to length of palatal shelf	0.491±0.101	0.475±0.075	0.454±0.119	0.532±0.086	0.561±0.194	0.519±0.189	0.544±0.061

Results represent Mean ± SD (*, $p \leq 0.05$; **, $p \leq 0.01$ compared with the groups treated with control retrovirus for each corresponding titer. See Table 5).

Table 7 Effects of *Hoxa2* antisense retrovirus treatment on cultured mouse palates

	Titer (cfu/ml)	0.016×10^5 (n=22-24)	0.08×10^5 (n=19-22)	0.4×10^5 (n=16-22)	0.8×10^5 (n=18-22)	1.6×10^5 (n=20-21)	2.4×10^5 (n=17-21)	3.2×10^5 (n=16-21)
***Hoxa2* Antisense Retrovirus**	**Length of palatal shelf (mm)**	1.302±0.217	1.260±0.050*	1.257±0.047*	1.359±0.153*	1.332±0.074*	1.266±0.096**	1.294±0.043
	Length of fused portion (mm)	0.588±0.203	0.724±0.190*	0.618±0.112	0.944±0.118*	0.917±0.119*	0.939±0.120*	0.919±0.155*
	Ratio of length of fused portion to length of palatal shelf	0.477±0.143	0.568±0.124*	0.496±0.104	0.651±0.065*	0.670±0.073*	0.732±0.099*	0.706±0.125*

Results represent Mean ± SD (*, $p \leq 0.05$; **, $p \leq 0.01$ compared with the groups treated with control retrovirus for each corresponding titer. See Table 5).

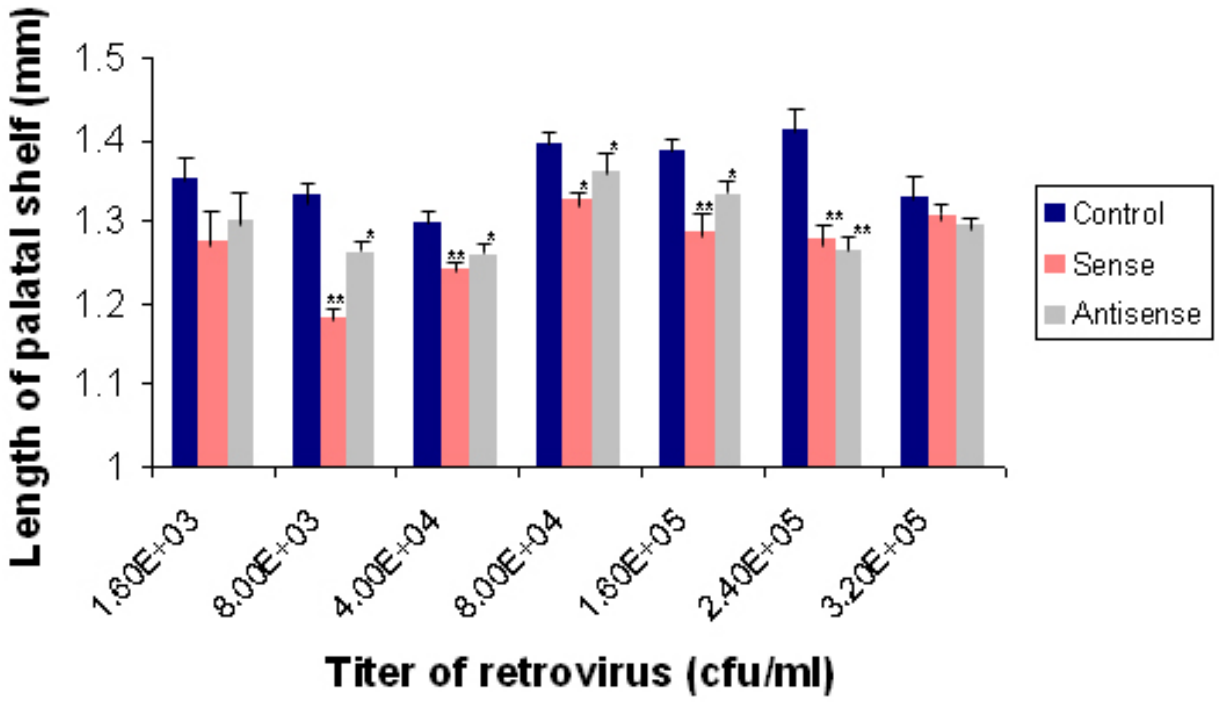

Figure 11 Comparison of length of palatal shelf in each titer group treated with control retrovirus, *Hoxa2* sense and antisense retrovirus, respectively. Bar chart represents Mean ± SD (*, $p \leq 0.05$; **, $p \leq 0.01$ compared with the groups treated with control retrovirus for each corresponding titer).

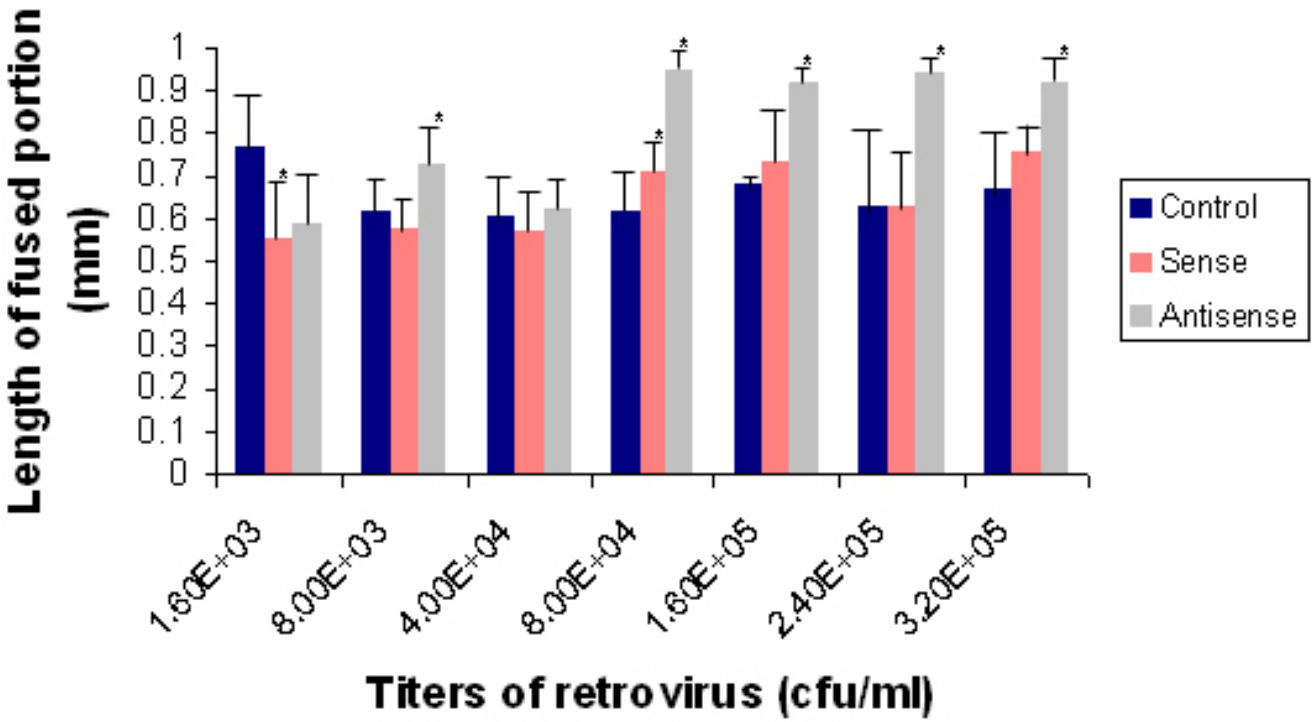

Figure 12 Comparison of length of fused portion in each titer group treated with control retrovirus, *Hoxa2* sense and antisense retrovirus, respectively. Bar chart represents Mean ± SD (*, $p \leq 0.05$ compared with the groups treated with control retrovirus for each corresponding titer).

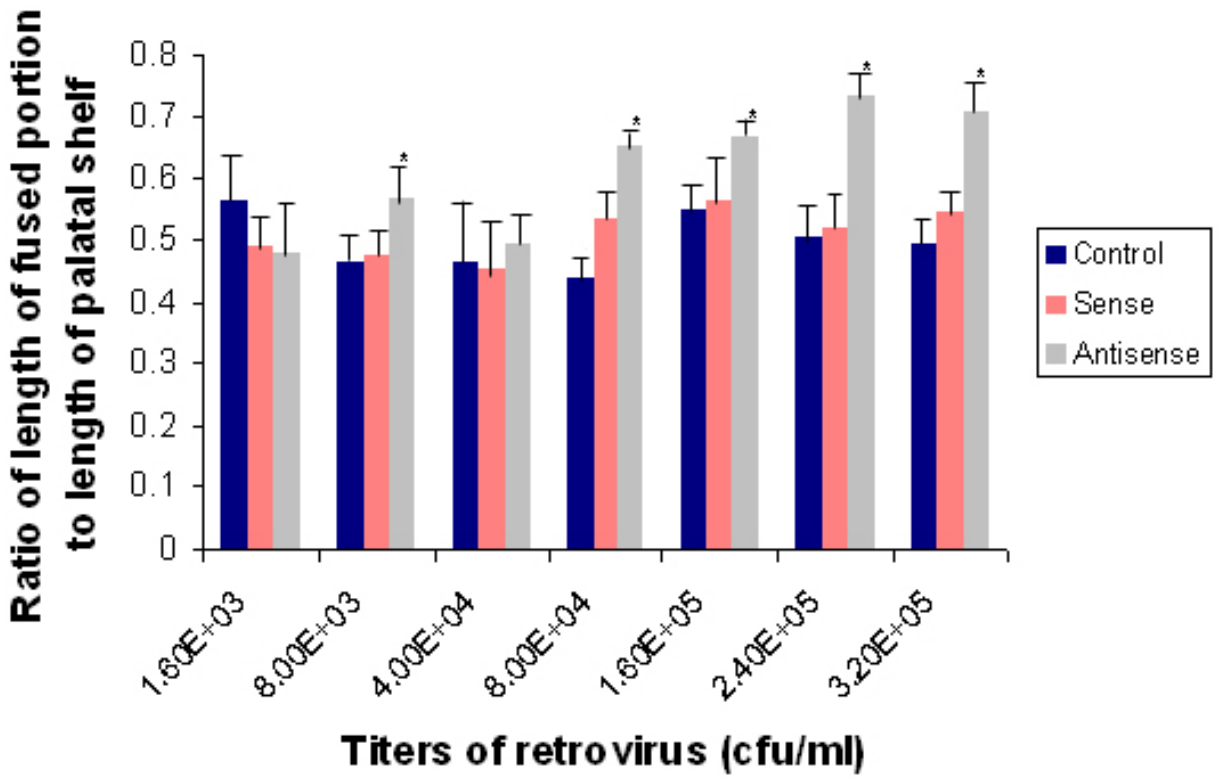

Figure 13 Comparison of ratio of length of fused portion to length of palatal shelf in each titer group treated with control retrovirus, *Hoxa2* sense and antisense retrovirus, respectively. Bar chart represents Mean ± SD (*, $p \leq 0.05$ compared with the groups treated with control retrovirus for each corresponding titer).

Table 8 Palate contact and fusion assessment after infection with control, *Hoxa2* sense and *Hoxa2* antisense retroviral particles

Titer (cfu/ml)		0.016×10^5	0.08×10^5	0.4×10^5	0.8×10^5	1.6×10^5	2.4×10^5	3.2×10^5
Control retrovirus	**Frequency of contacted palates (± fusion)**	86.4% (19/22)	86.4% (19/22)	85.0% (17/20)	77.3% (17/22)	90.0% (18/20)	83.3% (15/18)	81.0% (17/21)
	Frequency of fused palates	81.8% (18/22)	86.4% (19/22)	85.0% (17/20)	77.3% (17/22)	80.0% (16/20)	83.3% (15/18)	81.0% (17/21)
***Hoxa2* sense retrovirus**	**Frequency of contacted palates (± fusion)**	72.7% (16/22)	73.7% (14/19)	56.2% (9/16)	61.1% (11/18)	50.0% (10/20)	58.8% (10/17)	56.2% (9/16)
	Frequency of fused palates	72.7% (16/22)	42.1% (8/19)	43.8% (7/16)	44.4% (8/18)	45.0% (9/20)	41.2% (7/17)	50.0% (8/16)
***Hoxa2* antisense retrovirus**	**Frequency of contacted palates (± fusion)**	45.8% (11/24)	45.0% (10/22)	81.8% (18/22)	50.0% (10/20)	33.3% (7/21)	38.1% (8/21)	27.7% (5/18)
	Frequency of fused palates	45.8% (11/24)	40.9% (9/22)	46.1% (10/22)	45.0% (9/20)	33.3% (7/21)	38.1% (8/21)	27.7% (5/18)

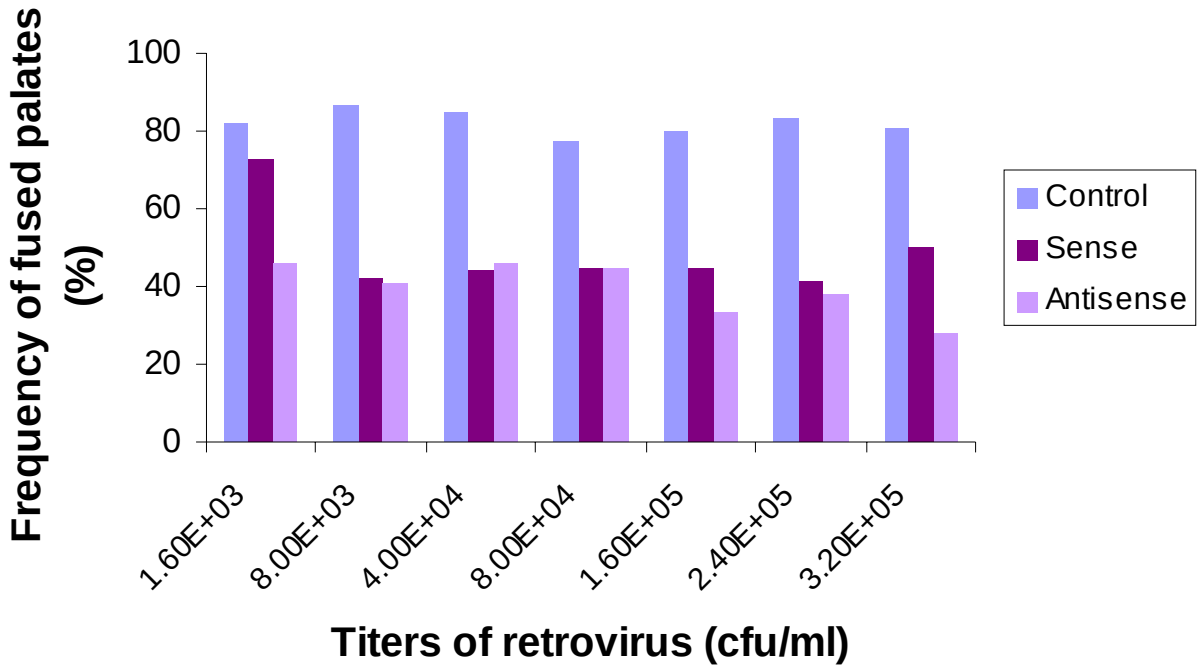

Figure 14 Comparison of frequency of fused palates in each titer group treated with control retrovirus, *Hoxa2* sense and antisense retrovirus, respectively.

6.5 *Hoxa2* mutant new born mice with cleft palates exhibit no defects in the origin of the hyoid and extrinsic tongue muscles

It has previously been reported that one of the extrinsic muscles of the tongue (hyoglossus) exhibits altered sites of origin in all the mutant classes lacking *Hoxa2* (Barrow and Capecchi, 1999). Histological analysis of the hyoid regions was performed to demonstrate the attachment of the hyoglossus muscle to the hyoid, both on a wild-type mouse without a cleft palate and a *Hoxa2* mutant mouse with a cleft palate. We found the hyoglossus was inserted in the greater horn of hyoid even in the *Hoxa2* mutant new born mouse with a cleft palate (N=1) (Fig. 15), which is consistent with the results reported by Ohnemus et al. (2001) (see Section 7, Discussion).

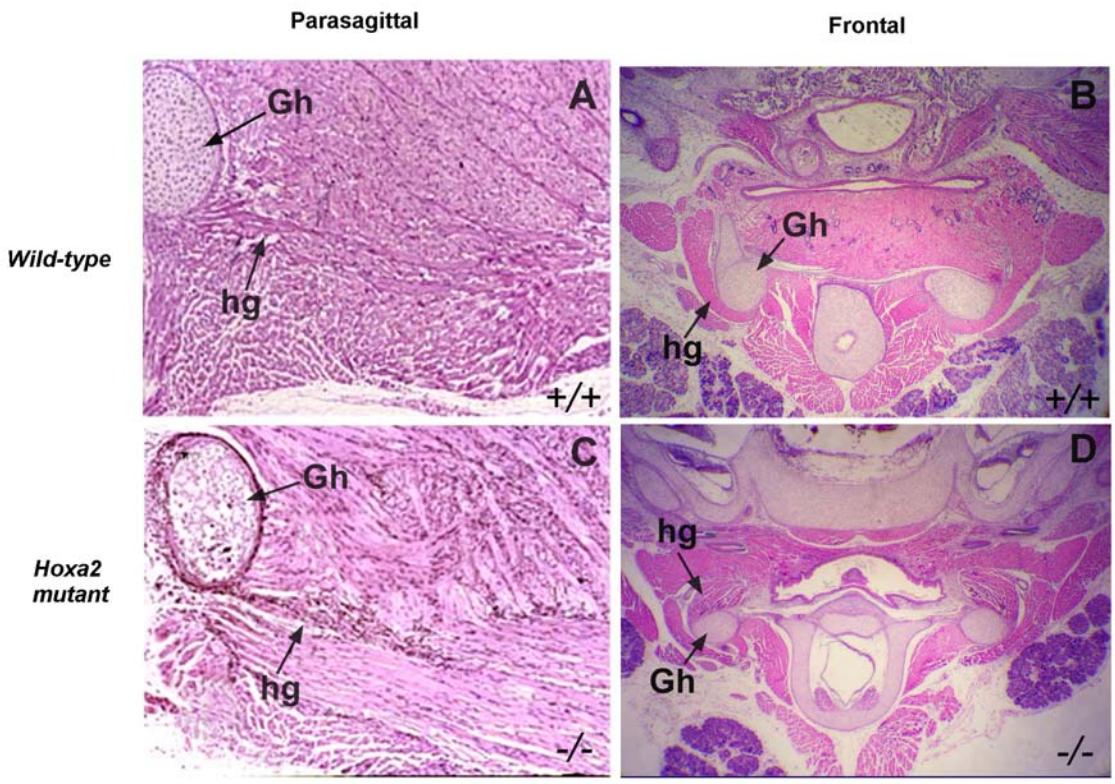

Figure 15 Histological analysis of the hyoid regions of new born mice with different *Hoxa2* genotypes. (A, C) Parasagittal sections of new born mice. (B, D) Frontal sections of new born mice, stained with Hematoxylin and Eosin. (A, B) In a wild-type new born mouse without a cleft palate, the hyoglossus (hg) attaches to the greater horn of the hyoid (Gh). (C, D) In a *Hoxa2* mutant mouse with a cleft palate, a similar situation was also observed that the hyoglossus (hg) inserts in the greater horn of hyoid (Gh).

7. Discussion

7.1 Cleft palate observed in *Hoxa2* mutant (*Hoxa2*$^{-/-}$) mice is not only a secondary effect caused by the abnormal tongue musculature.

Previous findings have indicated that *Hoxa2* null allele mice exhibit a cleft palate due to abnormal attachment of the hyoglossus muscle to the greater horn of the hyoid. This does not allow depression of lateral edges of the tongue resulting in a cleft secondary palate (Barrow and Capecchi, 1999). These studies suggest the importance of tongue posture in the elevation of palatal shelves. However, our laboratory has developed an *in vitro* whole organ palatal culture model where the tongue was removed. This model enabled us to investigate the role of *Hoxa2* in palate growth without any interference from the tongue (Zhang, W., M.Sc. Thesis, 2003). Subsequently, this study of whole organ palatal culture infected with pLEGFP-*Hoxa2* sense and antisense retrovirus demonstrates a low palatal fusion rate which is comparable with *Hoxa2*$^{-/-}$ mice (44.6%), by means of overexpression or inhibition of *Hoxa2* gene. These results, as well as an immunohistochemical study and *Hoxa2* expression by real-time RT-PCR indicate that the *Hoxa2* gene appears to have a direct role in palate formation.

Palate organ culture in vitro also shows the length of palatal shelf in *Hoxa2* mutant mice is smaller than their heterozygous and wild-type counterparts. This defect is observed in the groups treated with sense and antisense virus, suggesting either overexpression or inhibition of *Hoxa2* expression during palate development impacts the whole palate growth negatively. This impact on palatal shelf development as a result of altered *Hoxa2* expression further suggests that *Hoxa2* gene plays an essential role in regulating palatal growth. The low palatal fusion frequencies observed in both the virus

treated groups and *Hoxa2* mutant mice in comparison with the heterozygous and wild-type groups, may be primarily due to the smaller size of the palatal shelf, causing insufficient closure of the two palatal shelves. It may also be due to changes in cell apoptosis or cell proliferation, resulting in delayed palatal elevation and allowing the advancing developing tongue to interfere with palatal fusion.

7.2 The role of the tongue in palate development in *Hoxa2* mutant mice

It has been reported previously that *Hoxa2* mutants possess cleft palate at high penetrance (Gendron-Maguire et al., 1993; Rijli et al., 93; Barrow and Capecchi, 1999). *In vivo*, a cleft in the secondary palate in *Hoxa2* mutant mice is at 82 % penetrance reported by Rijli et al. (1993) and Barrow and Capecchi (1999). However, our *in vitro* palatal organ culture in which the tongue is removed at E12.5 exhibits a 55.4% penetrance of cleft palate in *Hoxa2* mutant mice. Here the significantly different penetrance of cleft palate may primarily be due to the role of the tongue in palate development in *Hoxa2* mutant mice.

Indeed, Barrow and Capecchi (1999) have found in *Hoxa2* mutant mice with a CLP, that the hyoglossus muscle was prevented from attaching to the greater horn of the hyoid bone, demonstrating that this defect occurs during palatal shelf closure. The hyoglossus functions to depress the lateral edges of the tongue. It is possible that, during embryogenesis, this extrinsic tongue muscle plays a vital role in flattening the tongue such that the flanking palatal shelves can lift and fuse above it (Barrow and Capecchil, 1999). In this case, if the hyoglossus does not attach to the greater horn of hyoid at E13.5 and E14.5, when the palate shelves start approaching each other to fuse, the delay of attachment of the hyloglossus muscle to the greater horn of the hyoid bone may cause the

tongue to adopt a posture which interferes with the lifting of the palatal shelves above the tongue, such that it obstructs palate shelf closure, resulting in a cleft palate. This role of the tongue may account for the difference in cleft palate observed *in vivo* and *in vitro*.

7.3 *Hoxa2* participates in epithelial-mesenchymal interactions during palatal shelf growth

The process of palate development can be divided into two stages: the growth of palatal shelves and the fusion of palatal shelves. The development of palatal shelves has been shown to require epithelial-mesenchymal interactions in order for secondary palate formation to take place. Tyler and Pratt (1980) indicate that oral and nasal regions of the palatal epithelium undergo limited differentiation when cultured alone, without epidermal growth factor (EGF). They were also the first to suggest that epithelial-mesenchymal interactions are required for palatal growth, and that the epithelium seems to require mesenchymal response to the mitogenic effects of EGF (Tyler and Pratt, 1980). Ferguson and Honig (Ferguson and Honig, 1984) in their studies established the critical role of epithelial-mesenchymal interactions and their timing during secondary palate development. Their work provided further evidence for the role of the mesenchyme in directing the fate of epithelial cells. In mice, both the mandibular and palatal epithelial cell fates are determined by E12, and the orientation of palatal mesenchyme seem to direct epithelial differentiation into nasal, oral, and medial edge epithelium (MEE) regions (Thesleff and Sharpe, 1997). The immunohistochemical study (Zhang, W., M.Sc. Thesis, 2003) and real-time RT-PCR experimental results show that *Hoxa2* in palatal shelves is expressed at E12.5, and increases from E12.5 to E13.5. The distribution of expression is localized in oral and nasal epithelia and, especially strong *Hoxa2* expression

is visible in the anterior mesenchymal region of the palatal shelves. These results appear to be precisely coordinated with the epithelial-mesenchyme interactions in the palatal growth process. These data provides new evidence for the role of *Hoxa2* in regulation of palatal shelf growth by its participation in epithelial-mesenchyme interactions and suggests a mechanism by which *Hoxa2* regulates the proliferation and reprogramming of the mesenchyme, which consequently directs the fate of epithelial cells. The high level of *Hoxa2* expression and the significant outgrowth of the palatal shelves, which both occur between 12.5 to E13.5 suggest that *Hoxa2* may play a key role during epithelial-mesenchyme interactions. However, it has yet to be elucidated whether *Hoxa2* governs this process directly or through indirect interaction with other genes.

7.4 *Hoxa2* regulates palatal fusion

The palate epithelium can be divided into three regions: the nasal, oral, and medial edge epithelium (MEE) The fusion of palatal shelves involves adhesion, migration, apoptosis and transdifferentiation of MEE cells into mesenchymal cells.

Previous immunohistochemical results (Zhang, W., M.Sc. Thesis, 2003) conducted in our laboratory show that at the palatal fusion stage, from E14 to E14.5, expression of *Hoxa2* was pronounced in MEE. Our assessment of palatal fusion shows the length of the fused palatal shelves in palates treated with antisense virus increased as the titer of virus increased. This suggests that *Hoxa2* may play a role in regulating the transdifferentiation of epithelium cells in the MEE region. That may also imply a pathway for *Hoxa2* to directly inhibit the downstream regulation of target genes allowing the epithelial cells in MEE to proliferate and induce fusion in the palatal shelves.

Recently, some of the molecular signaling pathways involved in the epithelial-mesenchymal interactions have been unraveled. The importance of Transforming Growth Factors (*TGFβs*) signaling during palatogenesis was further emphasized in a study by other researchers (Ito et al., 2003). *TGFβ3* is expressed both in the MEE cells and in the mesenchyme adjacent to MEE during secondary palate development. It is localized predominantly in the epithelium covering the palatal shelves which includes the palatal oral epithelium, palatal nasal epithelium and MEE before and during palatal shelf contact at the midline at E14.5 (Cui et al., 2003; Cui and Shuler, 2000; Cui et al., 1998). It has been reported that *TGFβ3* plays an important role in the events regulating the disappearance of MEE during palatal fusion. *TGFβ3* is the only gene that exhibits a partial or complete cleft palate in null-allele mice that is not associated with other craniofacial abnormalities (Kaartinen et al., 1995; Proetzel et al., 1995). Therefore, it is possible that *TGFβ3* may in fact be the direct downstream target gene of *Hoxa2*.

7.5 Initiation of *Hoxa2* gene expression in first branchial arch derivatives

During craniofacial development, neural crest cells migrate into the branchial arches to form the skeletogenic elements (Noden, 1982; Noden, 1983). The development of vertebrate branchial arches is regulated in several stages, during which global and local patterning events and different cellular populations participate in the branchial arch development. As branchial arches of vertebrate embryos are transient structures (Trokovic et al., 2002), the first arch subsequently subdivides into maxillary and mandibular portions. The maxillary prominence contributes to formation of the upper midface and palate through interactions with the frontonasal prominence (Cai et al., 2005). In mouse embryos, the secondary palate develops initially, as an outgrowth of the

maxillary prominences, at embryonic day (E) 11.5 (Murray and Schutte, 2004). Recent evidence suggests that in addition to neural crest cells, cells from all three germ layers contribute to the development and patterning of the branchial arches. Neural crest cells normally give rise to the patterned skeletal derivatives of the branchial arches (Trokovic et al., 2002), while the cranial mesoderm forms the predominantly myogenic cores of each branchial arch (Noden, 1986; Noden, 1987), maintaining an anterior-posterior register between these different primordial elements (Trainor and Tam, 1995). The endoderm is shown to be responsible for promoting the formation of branchial arch components in amphibians by directing neural crest cells towards a chondrogenic fate (Epperlein, 1974). The ectoderm surface also plays an important role in patterning the branchial arch derivatives (Trainor and Krumlauf, 2001). Recently, non-neural crest cell types have been shown to have an important role in controlling the fate of neural crest cells, and in regulating regional characteristics of branchial components other than neural crest cells (Trokovic et al., 2002). However, very little is known about the mechanisms involved. Previous studies have indicated that the expression domain of *Hoxa2* extends to the r1/r2 junction, although there is no *Hoxa2* gene expression in migrating neural crest cell from r1/r2 into the first branchial arch (Prince and Lumsden, 1994; Rijli et al., 1993).

The real-time RT-PCR results have demonstrated, however, that *Hoxa2* is expressed in the palatal shelves as early as E12.5. Since the first branchial arch (composed of crest cells from r1 and r2 of hindbrain and midbrain) is completely devoid of *Hoxa2* gene expression (Kontges and Lumsden, 1996), a question raised can be: How is *Hoxa2* expression triggered as the palatal shelves grow from the neural crest-derived first arch? Two possible mechanisms may be involved: the first may involve interactions between

neural crest and non-neural crest cells, enabling the neural crest cells to respond to environment signals and in turn switch on *Hoxa2* gene expression during the first arch development. The second mechanism may involve activation by upstream *Hox* genes or growth factors within the neural crest cells. On the basis of the expression patterns of signaling molecules expressed in distinct regions of the branchial ectoderm and endoderm, we can speculate that these neural crest dependent mechanisms may involve endothelins, bone morphogenetic proteins, Wnt family members, Sonic Hedgehog, several members of the FGF family (Francis-West et al., 1998), and the class II homeobox gene Msx2 (Winograd et al., 1997) expressed in migrating neural crest cells.

Further experiments by other researchers have also showed that signals from the ventral forgut endoderm specify the position that is adopted by facial cartilages with respect to the body axis (Couly et al., 2002). *Hox*-expressing neural crest cells are similarly responsive to endodermal cues arising from the more caudal part of the foregut endoderm (Ruhin et al., 2003). Experiments on pharyngeal endoderm have provided a profound influence on the morphogenesis of the middle and lower face (Crump et al., 2004a; Crump et al., 2004b; Trokovic et al., 2003; Veitch et al., 1999). Recent work shows that Fgf signaling is essential for this tissue patterning (Crump et al., 2004a).

More recently, an interesting study pointed a *Hox/Pbx* response element (E2-A2RE) that is critical for the *Hoxa2*-mediated activation of enhancer 2 (E2), and this activation of E2 by *Hoxa2* may imply that this gene is locally self-regulated (Lampe et al., 2004).

7.6 Signaling pathways in palate development

Msx1 is expressed in the anterior mesenchyme of the developing palate from E11.5 to E13.5 (Zhang et al., 2002). In the *Msx1* null mutant embryos the paired palatal shelves

elevate normally but fail to make contact and fuse (Satokata and Maas, 1994). This failed fusion between the palatal shelves of *Msx1-/-* embryos is the result of significantly lower levels of cell proliferation in their anterior region leading to growth impairment (Zhang et al., 2002). When *Msx1*-deficient palatal shelves were placed in contact with each other in organ culture, the shelves fused indicating that this was not the cause of the cleft palate. Examination of gene expression levels of E13.5 *Msx1* mutant embryos revealed a direct significant downregulation of *Bmp4* levels in the palatal mesenchyme, while its effects on *Shh* in the MEE and *Bmp2* in both the epithelium and mesenchyme are indirect (Zhang et al., 2002). Interestingly, even though *Msx1*, *Bmp2*, *Bmp4*, and *shh* were found to be expressed only in the anterior region of the palatal shelves at E12.5 and E13.5, posterior regions were also affected. That disruption of this signaling network leads to cleft palate (Zhang et al. 2002). *Hoxa2* gene has been shown to be expressed along the antero-posterior axis in both the epithelium and the mesenchyme of palatal shelves from E12 to E13.5 and especially has the highest intensity in the anterior mesenchyme at E13.5 (Zhang W, M.Sc. Thesis, 2003). This implies that *Hoxa2* may participate and drive the epithelium and mesenchyme interactions that support cell proliferation and palate growth in this signaling pathway.

Palatal mesenchyme expresses *Bmp4*, and that ectopic BMP4 protein induces expression of *Shh* in palatal epithelium. Ectopic Shh protein induces the expression of *Bmp2* in the mesenchyme, thus indicating that *Shh* signals from the epithelium back to mesenchyme. *Bmp2* then acts as a mitogen to stimulate proliferation in the mesenchyme. A similar signaling network has been established previously for tooth development (Bei et al., 2000; chen et al., 1996; Dassule et al., 2000; Gritli-Linde et al., 2002). Work by

Thesleff and Sharpe (1997), has shown that *Shh* is expressed along the entire anteroposterior axis of palatal epithelium at E13 (Keranen et al., 1999), and that mesenchymal *Fgf10* regulates epithelial expression of *Shh* through epithelial receptor Fgfr2b. It is possible that the expression of *Shh* is under complex regulation where *Bmp* signaling primarily regulates the anterior expression of *Shh*, and *Fgf* signaling along the whole anterior-posterior length of the MEE (Bei and Maas, 1998). We do not know if *Hoxa2* is involved in these signaling pathways, and further experiments are needed to determine the role of *Hoxa2* in palate signaling events.

8. Conclusion

In this study, the expression of *Hoxa2* gene in wild-type developing palates was quantified with real-time RT-PCR from E12.5 to E15.5. The relative overall expression of *Hoxa2* gene in the developing palate was the highest at E12.5, but decreased at E13.5 to E15.5. The effect on *Hoxa2* gene expression in palatal shelves after treatment with *Hoxa2* sense, *Hoxa2* antisense or control retroviral particles was also quantified with real-time RT-PCR and the corresponding protein expression level was detected by western blot analysis. Results demonstrate that *Hoxa2* gene expression in palatal shelves is enhanced by infection with *Hoxa2* sense retrovirus and suppressed by infection with *Hoxa2* antisense retrovirus. In addition, the length of palatal shelves and the palate fusion rates were evaluated in cultured palates treated with *Hoxa2* sense or antisense retroviral particles. Results show that in most titer groups (*Hoxa2* sense: 0.08×10^5 - 3.2×10^5 cfu/ml; *Hoxa2* antisense: 0.016×10^5 - 3.2×10^5 cfu/ml), retrovirus expressing either sense *Hoxa2* or antisense *Hoxa2* transcripts could inhibit palatal development and, subsequently, induce a low fusion rate of secondary palates (27.7%-50%), implicating a direct role of *Hoxa2* gene in the palatal development. Our results demonstrate for the first time that direct interference of *Hoxa2* transcripts in the developing palate affects palatal development.

The quantitative real-time RT-PCR results of *Hoxa2* mRNA in palatal shelves and the measured effects on palate growth and fusion rates after retroviral (sense and antisense *Hoxa2*) infection, as well as the previous immunohistochemical studies (Zhang, W., M.Sc. Thesis, 2003), have provided a picture of a dynamic role of *Hoxa2* gene during palate development. From E12.5 to E13.5, *Hoxa2* expresses mainly in the anterior mesenchymal

region of the palatal shelf and may direct the proliferation and reprogramming of the epithelial cells in the oral and nasal region. At this point, it may play a role in palatal outgrowth. From E14.5 to E15.5, *Hoxa2* expression levels decreased in the mesenchyme and the expression was restricted to the medial epithelial region (Zhang W, M.Sc. Thesis, 2003). Hence, *Hoxa2* gene's role may change from regulation of palatal shelf growth to the regulation of palatal shelf fusion. If *Hoxa2* gene is involved in the regulation of the palatal outgrowth, it can be concluded that overexpression or inhibition of *Hoxa2* expression can induce a low frequency of palatal fusion. Indeed, this is what has been demonstrated in this study. In the process of palatal fusion, *Hoxa2* may inhibit downstream target gene in wild-type palates, leading to a regulation of epithelial migration, apoptosis or the transdifferentiation of medial edge epithelial cells into mesenchymal cells. It is interesting to speculate that this target gene candidate may be *TGFβ3*. From observing the effect of *Hoxa2* sense and antisense retrovirus on palatal shelves, it appears that the *Hoxa2* gene has a greater impact on palatal shelf growth than it does on palatal shelf fusion.

9. References

Abbott, B. D., and Buckalew, A. R. (1992). Embryonic palatal responses to teratogens in serum-free organ culture. *Teratology* **45,** 369-382.

Abbott, B. D., Held, G. A., Wood, C. R., Buckalew, A. R., Brown, J. G., and Schmid, J. (1999). AhR, ARNT, and CYP1A1 mRNA quantitation in cultured human embryonic palates exposed to TCDD and comparison with mouse palate in vivo and in culture. *Toxicol. Sci.* **47,** 62-75.

Abu-Issa, R., Smyth, G., Smoak, I., Yamamura, K., and Meyers, E. N. (2002). Fgf8 is required for pharyngeal arch and cardiovascular development in the mouse. *Development* **129,** 4613-4625.

Andersen, H., and Matthiessen, M. (1967). Histochemistry of the early development of the human central face and nasal cavity with special reference to the movements and fusion of the palatine processes. *Acta Anat* **68,** 473-508.

Andres, G. (1949). Untersuchungen an chimaren von Triton und Bombinator. *Genetics* **24,** 387.

Babiarz, B. S., Allenspach, A. L., and Zimmerman, E. F. (1975). Ultrastructural evidence of contractile systems in mouse palates prior to rotation. *Dev. Biol* **47,** 32-44.

Babiarz, B. S., Wee, E. L., and Zimmerman, E. F. (1979). Palate morphogenesis III. Changes in cell shape and orientation during shelf elevation. *Teratology* **20,** 249-278.

Barrow, J. R., and Capecchi, M. R. (1999). Compensary defects associated with mutations in Hoxa1 restore normal palatogenesis to Hoxa2 mutants. *Developpment* **126,** 5011-5026.

Barrow, J. R., Stadler, H. S., and Capecchi, M. R. (2000). Roles of Hoxa1 and Hoxa2 in patterning the early hindbrain of the mouse. *Development* **127,** 933-944.

Been, W., and Song, S. (1978). Harelip and cleft palate conditions in chick embryos following local destruction of the mesencephalic neural crest. A preliminary note. *Acta Morphol Neer-scand.* **16,** 245-255.

Bei, M., Kratochwil, K., and Maas, R. L. (2000). BMP4 rescues a non-cell-autonomous function of Msx1 in tooth development. *Development* **127,** 4711-4718.

Bei, M., and Maas, R. (1998). FGFs and BMP4 induce both Msx1-independent and Msx-dependent signaling pathways in early tooth development. *Development* **125,** 4325-4333.

Ben-Khaial, G. S., and Shah, R. M. (1994). Effects of 5-fluorouracil on collagen synthesis in the developing palate of hamster. *Anti-Cancer Drugs* **5,** 99-104.

Berkovitz, B. K. B., Holland, G. R., and Moxham, B. J. (2002). Oral Anatomy, Histology and Embryology. *Mosby, Edinburgh*.

Birgbauer, E., and Fraser, S. E. (1994). Violation of cell lineage restriction compartments in the chick hindbrain. *Development* **120,** 1347-1356.

Blavier, L., Lazaryev, A., Groffen, J., Heisterkamp, N., DeClerck, Y. A., and Kaartinen, V. (2001). TGF-beta-3-induced palatogenesis requires matrix metalloproteinases. *Mol. Biol. Cell* **12,** 1457-1466.

Bobola, N., Carapuco, M., Ohnemus, S., Kanzier, B., Leibbrandt, A., Neubuser, A., Drouin, J., and Mallo, M. (2003). Mesenchymal patterning by Hoxa2 requires blocking Fgf-dependent activation of Ptx1. *Development* **130,** 3403-3414.

Bourguignon, L. Y. W., Zhu, H., Chu, A., Iida, N., Zhang, L., and Hung, M. C. (1997). Interaction between the adhesion receptor, CD44 and the oncogene product, p185HER2, promotes human ovarian tumor cell activation. *J Biol Chem.* **272,** 27913-27918.

Brinkley, L. L. (1980). In vitro studies of palatal shelf elevation. *In: Pratt, R. M., Christiansen, R. L. (eds). Current Research Trends in Prenatal Craniofacial Development***,** 203-220.

Brinkley, L. L., and Bookstein, F. L. (1986). Cell distribution during mouse secondary palatal closure II. Mesenchymal cells. *J Embryol Exp Morphol* **96,** 111-130.

Brinkley, L. L., and Morris-Wiman, J. (1984). Role of extracellular matrices in palatal shelf closure. *Current Topics in Developmental Biology* **19,** 17-36.

Brinkley, L. L., and Morris-Wiman, J. (1987). Computer-assisted analysis of hyaluronate distribution during morphogenesis of the mouse secondary palate. *Development* **100,** 629-636.

Bulliet, R. F., and Zimmermann, E. F. (1985). The influence of the epithelium on palate shelf reorientation. *J Embryol Exp Morphol* **88,** 265-279.

Burdi, A. R., and Faist, K. (1967). Morphogenesis of the palate in normal human embryos with special emphasis on the mechanisms involved. *Am J Anat.* **120,** 149-160.

Cai, J. L., Ash, D., Kotch, L. E., Jabs, E. W., Attie-Bitach, T., Auge, J., Mattei, G., Etchevers, H., Vekemans, M., Korshunova, Y., Tidwell, R., Messina, D. N., Winston, J. B., and Lovett, M. (2005). Gene expression in pharyngeal arch 1 during human embryonic development. *Human Molecular Genetics* **14,** 903-912.

Carette, M. J., and Ferguson, M. W. (1992). The fate of medial edge epithelial cells during palatal fusion in vitro: An analysis by Dil labelling and confocal microscopy. *Development* **114,** 379-388.

Chai, Y., Jiang, X., Ito, Y., Bringas, P., Jr., Han, J., Rowitch, D. H., Soriano, P., McMahon, A. P., and Sucov, H. M. (2000). Fate of the mammalian cranial neural crest during tooth and mandibular morphogenesis. *Development* **127,** 1671-1679.

Chen, y., Bei, M., woo, I., Satokata, I., and Maas, R. (1996). Msx1 controls inductive signling in mammalian tooth morphogenesis. *Development* **122,** 3035-3044.

Clarke, J. D., and Lumsden, A. (1993). Segmental repetition of neuronal phenotype sets in the chick embryo hindbrain. *Development* **118,** 151-162.

Cobourne, M. (2000). Construction for the modern head: current concepts in craniofacial development. *Journal of Orthodontics* **27,** 307-314.

Couly, G., Creuzet, S., Bennaceur, S., Vincent, C., and le Douarin, N. M. (2002). Interations between Hox-negative cephalic neural crest and the foregut endoderm in patterning the facial skeleton in the vertebrate head. *Development* **129,** 1061-1073.

Couly, G. F., Coltey, P. M., and Le Douarin, N. M. (1992). The developmental fate of the cephalic mesoderm in quail-chick chimeras. *Development* **114,** 1-15.

Cousley, R. R. J., and Roberts-Harry, D. (2000). An audit of the Yorkshire regional cleft database. *Journal of Orthodontics* 27, 319-322.

Creuzet, S., Couly, G., Vincent, C., and LeDouarin, N. M. (2002). Negative effect of Hox gene expression on the development of the neural crest-derived facial skeleton. *Development* **129,** 4301-4313.

Crump, J. G., Maves, L., Lawson, N. D., Weinstein, B. M., and Kimmel, C. B. (2004a). An essential role for Fgfs in endodermal pouch formation influences later craniofacial skeletal patterning. *Development* **131,** 5703-5716.

Crump, J. G., Swartz, M. E., and Kimmel, C. B. (2004b). An integrin-dependent role of pouch endoderm in hyoid cartilage development. *PLoS Biol.* **2,** E244.

Cserjesi, P., Lilly, B., Bryson, L., Wang, Y., Sassoon, D. A., and Olsen, E. N. (1992). Mhox: a mesodermally restricted homeodomain protein that binds an essential site in a muscle creatine kinase enhancer. *Development* **115,** 1087-1101.

Cuervo, R., and Covarrubias, L. (2004). Death is the major fate of medial edge epithelial cells and the cause of basal lamina degradation during palatogenesis. *Development* **131,** 15-24.

Cuervo, R., Valencia, C., Chandraratna, R. A. S., and Covarrubias, L. (2002). Programmed cell death is required for palate shelf fusion and is regulated by retinoic acid. *Dev. Biol* **245,** 145-156.

Cui, X.-M., Chai, Y., Chen, J., Yamamoto, T., Ito, Y., Bringas, P., and Shuler, C. F. (2003). TGF-beta3-dependent SMAD2 phosphorylation and inhibition of MEE proliferation during palatal fusion. *Dev.Dyn.* **227,** 387-394.

Cui, X.-M., and Shuler, C. F. (2000). The TGF-B type III receptor is localized to the medial edge epithelium during palatal fusion. *Int. J. Dev. Biol* **44,** 397-402.

Cui, X.-M., Warburton, D., Zhao, J. S., Crowe, D. L., and Shuler, C. F. (1998). Immunohistochemical localization of TGF-B type II receptor and TGF-B3 during palatogenesis in vivo and in vitro. *Int. J. Dev. Biol* **42,** 817-820.

Dassule, H. R., Lewis, P., Bei, M., Maas, R., and McMahon, A. P. (2000). Sonic hedgehog regulates growth and morphogenesis of the tooth. *Development* **127,** 4775-4785.

Davenne, M., Maconochie, M. K., Neun, R., Pattyn, A., Chambon, P., Krumlauf, R., and Rijli, F. M. (1999). Hoxa2 and Hoxb2 control dorsoventral patterns of neuronal development in the rostral hindbrain. *Neuron* **22,** 677-691.

De Angelis, V., and Nalbandian, J. (1968). Ultrastructure of mouse and rat palatal processes prior to and during secondary palate formation. *Archs Oral Biol.* **13,** 601-608.

Diewert, V. M. (1978). A quantitative coronal plane evaluation of craniofacial growth and spatial relations during secondary palate development in the rat. *Arch Oral Biol.* **23,** 607-629.

Diewert, V. M. (1980). Differential changes in cartilage cell proliferation and cell density in the rat craniofacial complex during secondary palate development. *Anat Rec* **198,** 219-228.

Diewert, V. M. (1983). A morphometric analysis of craniofacial growth and changes in spatial relations during secondary palatal development in human embryos and fetuses. *Am J Anat.* **167,** 495-522.

Diewert, V. M., and Wang, K. Y. (1992). Recent advances in primary palate and midface morphogenesis research. *Crit Rev Oral Biol Med* **4**. 111-130.

Dolle, P., Izpisua-Belmonte, J. C., Falkenstein, H., Renucci, A., and Duboule, D. (1989). Co-ordinate expression of the murine Hox-5 complex homeobox-containing genes during limb pattern formation. *Nature* **342,** 767-772.

Duboule, D., and Dolle, P. (1989). The structural and functional organization of the muring HOX gene family resembles that Drosophila homeotic genes. *EMBO J.* **8,** 1497-1505.

Dudas, M., and Kaartinen, V. (2005). TGF-beta superfamily and mouse craniofacial development: interplay of morphogenetic proteins and receptor signaling controls normal formation of the face. *Current Topics in Developmental Biology* **66,** 65-133.

Dudas, M., Sridurongrit, S., and Nagy, A. (2004). Craniofacial defects in mice lacking BMP type 1 receptors Alk2 in neural crest cells. *Mech Dev* **121,** 173-182.

Epperlein, H. H. (1974). The ectomesenchymal-endodermal interaction-system (EEIS) of Triturus al pestris in tissue culture. I. Observations on attachment, migration and differentiation of neural crest cells. *Differentiation* **2,** 151-168.

Farbman, A. I. (1968). Electron microscope study of palate fusion in mouse embryos. *Dev. Biol* **18,** 93-116.

Farlie, P. G., McKeown, S. J., and Newgreen, D. F. (2004). The neural crest: Basic bioloty and clinical relationships in the craniofacial and enteric nervous systems. *Birth Defects Res. Part C Embryo Today* **72,** 173-189.

Ferguson, M. W. (1988). Palate development. *Development* **103,** 41-60.

Ferguson, M. W., Honig, L. S., and Slavkin, H. C. (1984). Differentiation of cultured palatal shelves from alligator, chick, and mouse embryos. *Anat Rec* **209,** 231-249.

Ferguson, M. W. J. (1978). Palatal shelf elevation in the Wistar rat fetus. *J Anat.* **125,** 555-577.

Ferguson, M. W. J. (1981a). The structure and development of the palate in Alligator mississippiensis. *Archs Oral Biol.* **26,** 427-443.

Ferguson, M. W. J. (1981b). The value of the American alligator (Alligator mississippiensis) as a model for research in craniofacial development. *J. of Craniofac. Genet. Dev. Biol.* **1,** 123-144.

Ferguson, M. W. J. (1987). Palate development: mechanisms and malformations. *Irish J Med Sci.* **156,** 309-315.

Ferguson, M. W. J., and Honig, L. S. (1984). Epithelial-mesenchymal interactions during vertebrate palatogenesis. *Current Topics in Developmental Biology* **19,** 137-164.

Ferguson, M. W. J., and Honig, L. S. (1985). Experimental fusion of the naturally-cleft embryonic, chick palate. *J. of Craniofac. Genet. Dev. Biol.* **S1,** 323-337.

Fitchett, J. E., and Hay, E. D. (1989). Medial edge epithelium transforms to mesenchyme after embryonic palatal shelves fuse. *Dev. Biol* **131,** 455-474.

Fitzpatrick, D. R., Denhez, F., Kondaiah, P., and Akhurst, R. J. (1990). Differential expression of TGF beta isoforms in murine palatogenesis. *Development* **109,** 585-595.

Foreman, D. M., Sharpe, P. M., and Ferguson, M. W. J. (1991). Comparative biochemistry of mouse and chick secondary palate development in vivo and in vitro with particular emphasis on emphasis on extracellular matrix molecules and the effects of growth factors on their synthesis. *Archs Oral Biol.* **36,** 457-471.

Francis-West, P., Ladher, R., Barlow, A., and Graveson, A. (1998). Signalling interactions during facial development. *Mech. Dev* **75,** 3-28.

Francis-West, P. H., Robson, L., and Evans, D. J. (2003). Craniofacial development: The tissue and molecular interactions that control development of the head. *Adv. Anat. Embryol. Cell Biol.* **169,** 1-138.

Fraser, S., Keynes, R., and Lumsden, A. (1990). Segmentation in the chick embryo hindbrain is defined by cell lineage restriction. *Nature* **344,** 431-435.

Gammill, L. S., and Bronner-Fraser, M. (2003). Neural crest specification: migrating into genomics. *Nature Reviews Neuroscience* **4,** 795-805.

Gato, A., Martinez, M. L., Tudela, C., Alonso, I., Moro, J. A., Formoso, M. A., Ferguson, M. W., and Martinez-Alvarez, C. (2002). TGF-beta(3)-induced chondroitin sulphate proteoglycan mediates palatal shelf adhesion. *Dev. Biol.* **250,** 393-405.

Gaunt, S. J., Blum, M., and Robertis, E. M. D. (1993). Expression of the mouse goosecoid gene during mid-embryogenesis may mask mesenchymal lineages in the developing head, limbs and body wall. *Development* **117,** 769-778.

Gavalas, A., Davenne, M., Lumsden, A., Chambon, P., and Rijli, F. M. (1997). Role of Hoxa2 in axon pathfinding and rostral hindbrain patterning. *Development* **124,** 3693-3702.

Gendron-Maguire, M., Mallo, M. Z., Zhang, M., and Gridley, T. (1993). Hoxa-2 mutant mice exhibit Homeoic transformation of skeletal elements derived from cranial neural crest. *Cell* **75,** 1317-1331.

Glucksmann, A. (1965). Cell death in normal development. *Arch. Biol. (Liege)* **76,** 419-437.

Golding, J. P., Trainor, P., Krumlauf, R., and Gassmann, M. (2000). Defects in pathfinding by cranial neural crest cells in mice lacking the neuregulin receptor ErbB4. *Nat. Cell Biol.* **2,** 103-109.

Graham, A., Begbie, J., and McGonnell, I. (2004). Significance of the cranial neural crest. *Dev. Dyn* **229,** 5-13.

Grammatopoulos, G. A., Bell, E., Toole, L., Lumsden, A., and Tucker, A. S. (2000). Homeotic transformation of branchial arch identity after Hoxa2 overexpression. *Development* **127,** 5355-5365.

Greene, R. M., and Kochhar, D. M. (1974). Surface coat on the epithelium of developing palatine shelves in the mouse as revealed by electron microscopy. *J Embryol Exp Morphol* **31,** 683-692.

Greene, R. M., and Pratt, R. M. (1977). Inhibition by diazo-oxo-norlucine (DON) of rat palatal glycoprotein synthesis and epithelial cell adhesion in vitro. *Exp. Cell Res.* **105,** 27-37.

Griffin, G. J. (1984). Embryology of the central part of the face, closure of palate folds, and the maxillo-septal syndrome. *Austr Dent J* **29,** 15-26.

Griffith, C. M., and Hay, E. D. (1992). Epithelial-mesenchymal transformation during palatal fusion:carboxyfluorescein traces cells at light and electron microscopic levels. *Development* **116,** 1087-1099.

Gritli-Linde, A., Bei, M., Maas, R., zhang, X. M., Linde, A., and McMahon, A. P. (2002). Shh signaling within the dental epithelium is necessary for cell proliferation, growth and polarization. *Development* **129,** 5323-5337.

Guthrie, S., and Lumsden, A. (1991). Formation and regeneration of rhombomere boundaries in the developing chick hindbrain. *Development* **112,** 221-229.

Guthrie, S., Prince, V., and Lumsden, A. (1993). Selective dispersal of avian rhombomere cells in orthotopic and heterotopic grafts. *Development* **118,** 527-538.

Hao, Z., Yeung, J., Wolf, L., Doucette, R., and Nazarali, A. (1999). Differential Expression of Hoxa-2 protein along the dorsal-ventral axis of the development and adult mouse spinal cord. *Dev. Dyn* **216,** 201-217.

Helms, J. A., Cordero, D., and Tapadia, M. D. (2005). New insights into craniofacial morphogenesis. *Development* **132,** 851-861.

Helms, J. A., Kim, C. H., Hu, D., Minkoff, R., Thaller, C., and Eichele, G. (1997). Sonic hedgehog participates in craniofacial morphogenesis and is down-regulated by teratogenic doses of retinoic acid. *Dev. Biol.* **187,** 25-35.

Hunt, P., Clarke, J. D., Buxton, P., Ferretti, P., and Thorogood, P. (1998a). Segmentation, crest prespecification and the control of facial form. *Eur. J. Oral Sci* **106 Suppl. 1,** 12-18.

Hunt, P., Clarke, J. D., Buxton, P., Ferretti, P., and Thorogood, P. (1998b). Stability and plasticity of neural crest patterning and branchial arch Hox code after extensive cephalic crest rotation. *Dev. Biol* **198,** 82-104.

Hunt, P., Gulisano, M., Cook, M., Sham, M., Faiella, A., Wilkinson, D., Boncinelli, E., and Krumlauf, R. (1991a). A distinct Hox code for the branchial region of the vertebrate head. *Nature* **353,** 861-864.

Hunt, P., and Krumlauf, R. (1991). Deciphering the Hox code: clues to patterning branchial regions of the head. *Cell* **66,** 1075-1078.

Hunt, P., Whiting, J., Muchamore, I., Marshall, H., and Krumlauf, R. (1991b). Homeobox genes and models for patterning the hindbrain and branchial arches. *Development* **112 (Suppl.),** 187-196.

Innes, P. B. (1978). The ultrastructure of the mesenchymal element of the palatal shelves of the fetal mouse. *J Embryol Exp Morphol* **43,** 185-194.

Innes, P. B. (1981). The ultrastructure of murine secondary palatal ectomesenchyme during shelf reorientation. *J Craniofac Genet Dev Biol.* **1,** 359-371.

Innes, P. B. (1985). The ultrostructural effects of prednisolone on the mesenchyme of the palatal shelf in the mouse. *J Craniofac Genet Dev Biol.* **5,** 287-297.

Irving, C., and Mason, I. (2000). Signaling by FGF8 from the isthmus patterns anterior hindbrain and establishes the anterior limit of Hox gene expression. *Development* **127,** 177-186.

Itano, N., Sawai, T., Yoshida, M., Lenas, P., Yamada, Y., Imagawa, M., Shinomura, T., Hamaguchi, M., Yoshida, Y., Ohnuki, Y., Miyauchi, S., Spicer, A. P., McDonald, J. A., and Kimata, K. (1999). Three isoforms of mammalian hyaluronan synthases have distinct enzymatic properties. *J Biol Chem.* **274,** 25085-25092.

Ito, Y., Yeo, J. Y., Chytil, A., Han, J., Bringas, P., Jr., Nakajima, A., Shuler, C. F., Moses, H. L., and Chai, Y. (2003). conditional inactivation of Tgfbr2 in cranial neural crest causes cleft palate and calvarial defects. *Development* **130,** 5269-5280.

Johnston, M. C., and Sulik, K. K. (1990). In:Bhaskar S.N. (ed). Oral histology and embryology. *Mosby, London,* 12-16.

Kaartinen, V., Cui, X. M., Heisterkamp, N., Gropffen, J., and Shuler, C. F. (1997). Transforming Growth factor-â3 regulators transdifferentiation of mmedial edge

epithelium during palatal fusion and associated degradation of the basement membrane. *Dev. Dyn* **209,** 255-260.

Kaartinen, V., Voncken, J. W., Shuler, C., Warburton, D., Bu, D., N., H., and Croffen, J. (1995). Abnormal lung development and cleft palate in mice lacking TGF-â3 indicates defects of epithelium-mesenchymal interaction. *Nat. Genet* **11,** 415-421.

Kanzler, B., Kuschert, S. J., Liu, Y. H., and Mallo, M. (1998). Hoxa2 restricts the chondrogenic domain and inhibits bone formation during development of the branchial erea. *Development* **125,** 2587-2597.

Kappen, C., Schugart, K., and Ruddle, F. (1989). Two steps in the evolution of antennapedia-class vertebrate homeobox genes. *Proc. Natl. Acad. Sci. USA* **86,** 5459-5463.

Keranen, S. V., Kettunen, P., Aberg, T., Thesleff, I., and Jernvall, J. (1999). Gene expression patterns associated with suppression of odontogenesis in mouse and vole diastema regions. *Dev Genes Evol* **209,** 495-506.

Kessel, M., and Gruss, P. (1991). Homeotic transformations of murine prevertebrae and concommitant alteration of Hox codes induced by retinoic acid. *Cell* **67,** 89-104.

Kjaer, I. (1989). Prenatal skeletal maturation of the human maxilla. *J Craniofac Genet Dev Biol.* **9,** 257-264.

Koch, W. E., and Smiley, G. R. (1981). In vivo and in vitro studies of the development of the avian secondary palate. *Archs Oral Biol.* **26,** 181-187.

Kontges, G., and Lumsden, A. (1996). Rhombencephalic neural crest segmentation is preserved throughout craniofacial ontogeny. *Development* **122,** 3229-3242.

Krumlauf, R. (1993). Hox genes and pattern formation in the branchial region of the vertebrate head. *Trends Genet* **9,** 106-112.

Kuhn, E. M., Babiarz, B. S., Lessard, J. L., and Zimmerman, E. F. (1980). Palate morphogenesis 1. Immunological and ultrastructural analyses of mouse palate. *Teratology* **21,** 209-223.

Lampe, X., Picard, J., and Rezsohazy, R. (2004). The Hoxa2 enhancer 2 contains a critical Hoxa2 responsive regulatory element. *Biochemical and Biophysical Research Communications* **316,** 898-902.

Larson, W. J. (2001). *Human Embryology* **London, UK: Churchill Livingston**.

Larsson, K. S., Bostrom, H., and Carlsoo, S. (1959). Studies on the closure of the secondary palate. *Exp. Cell Res.* **16,** 379-383.

Le Douarin, N., and Kalcheim, C. (1999). The Neural Crest (eds, Bard, J., Barlow, P. & Kirk, D.). *Cambridge Univ. Press,* .

Lieb, R. J., and De Paola, D. P. (1981). Ultrastructural alteration of trypsin- and pancraetin- separated embryonic rabbit palate epithelium and mesenchyme. *J Dent Res.* **60,** 164-170.

Luke, D. A. (1976). Development of the secondary palate in man. *Acta Anat* **94,** 596-608.

Luke, D. A. (1984). Epithelial proliferation and development of rugae in relation to palatal shelf elevation in the mouse. *J Anat.* **138,** 251-258.

Lumsden, A., and Keynes, R. (1989). Segmental patterns of neuronal development in the chick hindbrain. *Nature* **337,** 424-428.

Lumsden, A., and Krumlauf, R. (1996). Patterning the vertebrate neuraxis. *Science* **274,** 1109-1115.

Lumsden, A., Sprawson, N., and Graham, A. (1991). Segmental origin and migration of neural crest cells in the hindbrain region of the chick embryo. *Development* **113,** 1281-1291.

MacKenzie, A., Ferguson, M. W. J., and Sharpe, P. T. (1991). Hox-7 expression during murine craniofacial development. *Development* **113,** 601-611.

Maconcochie, M., Krishnamurthy, R., Nonchev, S., Meier, P., Manzanares, M., Mitchell, P., and Krumlauf, R. (1999). Regulation of Hoxa2 in cranial neural crest cells involves members of the AP-2 family. *Development* **126,** 1483-1494.

Mallo, M., and Brandlin, I. (1997). Segmental identity can change independently in the hindbrain and rhombencephalic neural crest. *Dev. Dyn.* **210,** 146-156.

Marin, F., and Puelles, L. (1995). Morphological fate of rhombomeres in quail/chick chimeras: a segmental analysis of hindbrain nuclei. *Eur. J. Neurosci* **7,** 1714-1738.

Martinez-Alvarez, C., Blanco, M. J., Perez, R., Rabadan, M. A., Aparicio, M., Resel, E., Martinez, T., and Nieto, M. A. (2004). Snail family members and cell survival in physiological and pathological cleft palates. *Dev. Biol.* **265,** 207-218.

Martinez-Alvarez, C., Bonelli, R., Tudela, C., Gato, A., Mena, J., O'Kane, S., and Ferguson, M. W. (2000a). Bulging medial edge epithelial cells and palatal fusion. *Int. J. Dev. Biol* **44,** 331-335.

Martinez-Alvarez, C., Tudela, C., Perez- Miguelsanz, J., O'kane, S., Puerta, J., and Ferguson, W. J. (2000b). Medial edge epithelial cell fate during palatal fusion. *Dev. Biol* **220,** 343-357.

McGinnis, W., and Krumlauf, R. (1992). Homeobox gene and axial patterning. *Cell* **68,** 283-302.

McKee, C. M., Penno, M. B., Cowman, M., Burdick, M. D., Strieter, R. M., and Bao, C. (1996). Hyaluronan (HA) fragments induce chemokine gene expression in alveolar macrophages. *J Clin Invest.* **98,** 2403-2413.

Mclnnes, R. R., and Michaud, J. (2004). Developmental biology: Frontiers for clinical genetics. *Clin Genet* 65, 163-176.

Mohapatra, S., Yang, X., Wright, J. A., Turley, E. A., and Greenberg, A. H. (1996). Soluble hyaluronan receptor RHAMM induces mitotic arrest by suppressing Cdc2 and cyclin B1 expression. *J Exp Med.* **183,** 1663-1668.

Morgan, P. R., and Pratt, R. M. (1977). Ultrastructure of the expected fusion zone in rat fetuses with diazo-oxo-norleucine (DON) induced cleft palate. *Teratology* **15,** 281-290.

Mori, C., Nakamura, N., Okamoto, Y., Osawa, M., and Shiota, K. (1994). Cytochemical identification of programmed cell death in the fusing fetal mouse palate by specific labelling of DNA fragmentation. *Anat. Embryol. (Berl)* **190,** 21-28.

Moxham, B. J. (2003). The development of the palate-a brief review. *Eur. J. Anat.* . **7 Suppl,** 53-74.

Murray, J. C., and Schutte, B. C. (2004). Cleft palate:players, pathways, and pursuits. *J.Clin.Invest* **113,** 1676-1678.

Nawshad, A., and Hay, E. D. (2003). TGF beta3 signaling activates transcription of the LEF1 gene to induce epithelial mesenchymal transformation during mouse palate development. *J. Cell Biol.* **163,** 1291-1301.

Nawshad, A., LaGamba, D., and Hay, E. D. (2004). Transforming growth factor beta (TGFbeta) signalling in palatal growth, apoptosis and epithelial mesenchymal transformation (EMT). *Arch. Oral Biol.* **49,** 675-689.

Nazarali, A., Kim, Y., and Nirenberg, M. (1992). Hox-1.11 and Hox4.9 homeobox genes. *Proc. Natl. Acad. Sci. USA* **89,** 2883-2887.

Nazarali, A., Puthcode, R., Leung, V., Wolf, L., Hao, Z., and Yeung, J. (2000). Temporal and spatial expression of Hoxa-2 during murine palatogenesis. *Cellular and Molecular Neurobiology* **20,** 269-290.

Noble, P. W., McKee, C. M., and Horton, M. R. (1998). Induction of inflammatory gene expression by low molecular weight hyaluronan fragments in macrophages. *The Chemistry, Biology and Medical Applications of Hyaluronan and its derivatives,* 219-225.

Noden, D. M. (1978). The control of avian cephalic neural crest cytodifferentiation. I. Skeletal and connective tissues. *Dev. Biol.* **67,** 296-312.

Noden, D. M. (1982). Patterns and organization of craniofacial skeletogenic and myogenic mesenchyme: a perspective. *Prog Clin Biol Res* **101,** 167-203.

Noden, D. M. (1983). The role of the neural crest in pattering of avian cranial skeletal, connective, and muscle tissues. *Dev. Bio* **96,** 144-165.

Noden, D. M. (1986). Patterning of avian craniofacial muscles. *Dev. Bio* **116,** 347-356.

Noden, D. M. (1987). Interactions between cephalic neural crest and mesodermal populations. *In Developmental and Evolutionary Aspects of the Neural Crest. Edited by Maderson PFA. London: John wiley,* 89-119.

Noden, D. M. (1988). Interactions and fates of avian craniofacial mesenchyme. *Development* **103 (Suppl.),** 121-140.

Nonchev, S., Vesque, C., Maconochie, M., Seitanidou, T., Ariza-McNaughton, L., Frain, M., Marshall, H., Sham, M. H., Krumlauf, R., and Charnay, P. (1996). Segmental expression of Hoxa2 in the hindbrain is directly regulated by Krox-20. *Development* **122,** 543-554.

Ohnemus, S., Bobola, N., Kanzler, B., and Mallo, M. (2001). Different levels of Hoxa2 are requaired for particular developmental progress. *Mech. Dev* **108,** 135-147.

Pasqualetti, M., Ori, M., Nardi, I., and Rijli, F. M. (2000). Ectopic Hoxa2 induction after neural crest migration results in homeosis of jaw element in Xenopus. *Development* **127,** 5367-5378.

Pelton, R. W., Dickinson, M. E., Moses, H. L., and Hogan, B. L. (1990a). In situ hybridization analysis of TGF beta 3 RNA expression during mouse development: Comparative studies with TGF beta 1 and beta 2. *Development* **110,** 609-620.

Pelton, R. W., Hogan, B. L., Miller, D. A., and Moses, H. L. (1990b). Differential expression of genes encoding TGFs beta 1, beta 2 and beta 3 during murine palate formation. *Dev. Biol.* **141,** 456-460.

Pourtois, M. (1966). Onset of the acquired potentially for fusion in the palatal shelves of rats. *J. Embryol. Exp. Morphol.* **16,** 171-182.

Pratt, R. M., Goggins, J. F., Wilk, A. L., and King, C. T. G. (1973). Acid mucopolysaccharide synthesis in the secondary palate of the developing rat at the time of rotation and fusion. *Dev. Biol.* **32,** 230-237.

Pratt, R. M., and Hassell, J. R. (1975). Appearance and distribution of carbohydrate rich macromolecules on the epithelial surface of the rat palatal shelf. *Dev. Biol* **45,** 192-198.

Prince, V., and Lumsden, A. (1994). Hoxa2 expression in normal and transposed rhombomeres: independent regulation in the neural tube and neural crest. *Development* **120,** 911-923.

Proetzel, G., Pawlowski, S. A., Wiles, M. V., Yin, M., Boivin, G. P., Howles, P. N., Ding, J., Ferguson, M. W., and Doetschman, T. (1995). Transforming growth factor-beta 3 is required for secondary palate fusion. *Nat. Genet* **11,** 409-414.

Qiu, M., Bulfone, A., Ghattas, I., Meneses, J. J., Christensen, L., Sharpe, P. T., Presley, R., Petersen, R. A., and R., R. J. L. (1997). Role of the Dlx homeobox genes in proximodistal pattrening of the branchial arches: mutation of Dlx-1, Dlx-2, and Dlx-1 and -2 alter morphogenesis of proximal skeletal and soft tissue structures derived from the first and second arches. *Dev. Bio.* **185,** 165-184.

Qiu, M., Bulfone, A., Martinez, S., Meneses, J. J., Shimamura, K., Pedersen, R. A., and R., R. L. (1995). Null mutation of Dlx-2 results in abnormal morphogenesis of proximal first and second branchial arch derivatives and abnormal differentiation in the forebrain. *Genes Dev.* **9,** 2523-2538.

Rice, R., Spencer-Dene, B., Connor, E. C., Gritli-Linde, A., McMahon, A. P., Dickson, C., Thesleff, I., and Rice, D. P. (2004). Disruption of Fgf10/Fgfr2b-coordinated epithelial-mesenchymal interactions causes cleft palate. *J. Clin. Invest.* **113,** 1692-1700.

Richman, J. M., and Lee, S. H. (2003). About face: Signals and genes controlling jaw patterning and identity in vertebrates. *Bioessays* **25,** 554-568.

Rijli, F. M., Mark, M., Lakkaraju, S., Dierich, A., Dolle, P., and Chambon, P. (1993). A homeotic transformation is generated in the rostral branchial region of the head by disruption of Hoxa2, which acts as a selector gene. *Cell* **75,** 1333-1349.

Ruhin, B., Creuzet, S., Vincent, C., Benouaiche, L., Le Douarin, N. M., and Couly, G. (2003). Patterning of the hyoid cartilage depends upon signals arising from the vertral foregut endoderm. *Dev.Dyn.* **228,** 239-246.

Sadler, T. W. (2000). *Langman's Medical Embryology*, eighth edition, **Lippincott Williams and Wilkins, Philadelphia**, 370-375.

Satokata, I., and Maas, R. (1994). Msx1 deficient mice exhibit cleft palate and abnormalities of craniofacial and tooth development. *Nat. Genet.* **6,** 348-355.

Saunders, J. W., Jr. (1966). Death in embryonic systems. *Science* **154,** 604-612.

Schilling, T. F., Prince, V., and Ingham, P. W. (2001). Plasticity in Zebrafish hox expression in the hindbrain and cranial neural crest. *Dev. Bio* **231,** 201-216.

Schneider, R. A., and Helms, J. A. (2003). The cellular and molecular origins of beak morphology. *Science* **299,** 565-568.

Sechrist, J., Serbedzija, G. N., Scherson, T., Fraser, S. E., and Bronner-Fraser, M. (1993). Segmental migration of the hindbrain neural crest does not arise form its segmental generation. *Development* **118**.

Shah, N. M., Cheng, K. M., Suen, R., and Wong, A. (1985). An ultrastructural and histochemical study of the development of the secondary palate in Japanses quail. Coturnix coturnix japonica. *J. Craniofac. Genet. Dev. Biol.* **5,** 41-57.

Shah, R. M. (1979). Current concepts on the mechanisms of normal and abnormal secondary palate formation. *Advances in the Study of Birth Defects: Teratogenic mechanisms* **1,** 69-84.

Shah, R. M., Chen, Y. P., and Burdett, D. N. (1989). Effects of cylcophosphamide on the secondary palate development in Golden Syrian hamster: teratology, morphology and morphometry. *J Craniofac Genet Dev Biol.* **9,** 381-396.

Shah, R. M., Cheng, K. M., Suen, R., and Wong, A. (1987). Secondary palate development in the domestic duck (Khaki Campbell). An electron microscopic, histochemical, autoradiographic and biochemical study. *J. Anat.* **154,** 245-258.

Shah, R. M., and Crawford, B. J. (1980). Development of the secondary palate in chick embryo: a light and electron microscopic and histochemical study. *Invest Cell Pathol.* **3,** 319-328.

Shuler, C. F. (1995). Programmed cell death and cell transformation in craniofacial development. *Crit Rev Oral Biol Med* **6,** 202-217.

Shuler, C. F., Guo, Y., Majumder, A., and Luo, R. Y. (1991). Molecular and morphologic changes during the epithelia-mesenchymal transformation of palatal shelf medial edge epithelium in vitro. *Int. J. Dev. Biol* **35,** 463-472.

Shuler, C. F., Halpern, D. E., Guo, Y., and Sank, A. C. (1992). Medial edge epithelium fate traced by cell lineage analysis during epithelial-mesenchymal transformation in vivo. *Dev. Bio* **154,** 318-330.

Singh, G. D., and Moxham, B. J. (1993). Cellular activity in the developing palate of the rat assessed by straining of nucleolar organiser regions. *J Anat.* **182,** 163-168.

Singh, G. D., Moxham, B. J., Langley, M. S., and Embery, G. (1997).Glycosaminoglycan biosynthesis during 5-fluoro-2-deoxyuridine-induced palatal clefts in the rat. *Archs Oral Biol.* **42,** 355-363.

Singh, G. D., Moxham, B. J., Langley, M. S., Waddington, R. J., and Embery, G. (1994). Changes in the composition of glycosaminoglycans during normal palatogenesis in the rat. *Archs Oral Biol.* **39,** 401-407.

Souchon, R. (1975). Surface coat of the palatal shelf epithelium during palatogenesis in mouse embryos. *Anat Embryol.* **147,** 133-142.

Sperber, G. H. (1981). Craniofacial embryology. 28-50.

Sun, D., McAlmon, K. R., Davies, J. A., Bernfield, M., and Hay, E. D. (1998a). Simultaneous loss of expression of syndecan-1 and E-cadherin in the embryonic palate during epithelial-mesenchymal transformation. *Int. J. Dev. Biol* **42,** 733-736.

Sun, D. Z., Vanderburg, C. R., Odierna, G. S., and Hay, E. D. (1998b). TGF beta 3 promotes transformation of chicken palate medial edge epithelium to mesenchyme in vitro. *Development* **125,** 95-105.

Tan, D. P., Ferante, J., Nazarali, A., Shao, X., Kazak, C. A., Guo, V., and Nirenberg, M. (1992). Muring Hox1.11 homeobox gene structure and expression. *Proc. Natl. Acad. Sci. USA* **89,** 6280-6284.

Taniguchi, K., Sato, N., and Uchiyama, Y. (1995). Apoptosis and heterophagy of medial edge epithelial cells of the secondary palatine shelves during fusion. *Arch. Histol. Cytol.* **58,** 191-203.

Taya, Y., O'Kane, S., and J., F. M. W. (1999). Pathogenesis of palate in TGF-â3 knockout mice. *Development* **126,** 3869-3879.

Termeer, C. C., Hennies, J., Voith, U., Ahrens, T., Weiss, J., Prehm, P., and Simon, J. C. (2000). Oligosaccharides of hyaluronan are potent activators of dendritic cells. *J Immuno.* **165,** 1863-1870.

Thesleff, I., and Sharpe, P. (1997). Signaling networks regulating dental development. *Mech Dev* **67,** 111-123.

Thomas, S. (1999). Investigations into aspects of mammalian palatal development. *Ph.D. Thesis. Cardiff University*.

Toole, B. P. (2000). Hyaluronan is not just a goo. *J Clin Invest.* **106,** 335-336.

Trainor, P. (2003a). The bills of qucks and duails. *Science* **299,** 523-524.

Trainor, P. (2003b). Making headway: the roles of Hox genes and neural crest cells in craniofacial development. *The Scientific World Journal* **3,** 240-264.

Trainor, P., and Krumlauf, R. (2000). Plasticity in mouse neural crest cells reveals a new patterning role for cranial mesoderm. *Nat. Cell Biol.* **2,** 96-102.

Trainor, P., Manzanares, M., and Krumlauf, R. (2000). Genetic interactions during hindbrain segmentation in the mouse embryo. *In Mouse Brain Development:Results and Problems in Cell Differentiation* **30,** 51-89.

Trainor, P. A., Ariza-McNaughton, L., and Krumlauf, R. (2002). Role of the isthmus and FGFs in resolving the paradox of neural crest palsticity and prepatterning. *Science* **295,** 1288-1291.

Trainor, P. A., and Krumlauf, R. (2001). Hox genes, neural crest cells and branchial arch patterning. *Cell Prolif.* **13,** 698-705.

Trainor, P. A., and Tam, P. P. L. (1995). Cranial paraxial mesoderm and neural crest of the mouse embryo-codistribution in the craniofacial mesenchyme but distinct segregation in the branchial arches. *Development* **121,** 2569-2582.

Trokovic, N., Trokovic, R., Mai, P., and Partanen, J. (2003). Fgfr1 regulates patterning of the pharyngeal region. *Genes & Dev.* **17,** 141-153.

Trumpp, A., Depew, M. J., Rubenstein, J. L. R., Bishop, J. M., and Martin, G. R. (1999). Cre-mediated gene inactivation demonstrates that FGF8 is required for cell survival and patterning of the first branchial arch. *Genes & Dev.* **13,** 3136-3148.

Tucker, A. S., and Lumsden, A. (2004). Neural crest cells provide species-specific patterning information in the developing branchial skeleton. *Evol. Dev.* **6,** 32-40.

Tudela, C., Formoso, M. A., Martinea, T., Perez, R., Aparicio, M., Maestro, C., Del Rio, A., Martinez, E., Ferguson, M. W., and Martinez-Alvarez, C. (2002). TGF-beta3 is required for the adhesion and intercalation of medial edge epithelial cells during palate fusion. *Int. J. Dev. Biol* **46,** 333-336.

Tumpel, S., Maconcochie, M., Wiedemann, L. M., and Krumlauf, R. (2002). Conservation and diversity in the cis-regulatory networks that integrate information controlling expression of Hoxa2 in Hindbrain and cranial neural crest cell in vertebrates. *Dev. Biol.* **246**, 45-56.

Tyler, M. S., and Pratt, R. M. (1980). Effect of epidermal growth factor on secondary palatal epithelium in vitro: tissue isolation and recombination studies. *J Embryol Exp Morphol* **58,** 93-106.

Veitch, E., Begbie, J., Schilling, T. F., Smisth, M. M., and Graham, A. (1999). Pharyngeal arch patterning in the absence of neural crest. *Curr Biol* **9,** 1481-1484.

Wagner, G. (1959). Untersuchungen an Bombinator-Triton-Chimareren. *Roux Arch. Entwicklungsmech* **151,** 136-158.

Wee, E. L., Barbiarz, B. S., Zimmerman, S., and Zimmerman, E. F. (1979). Palate morphogenesis IV. Effects of serotonin and its antagonists on rotation in embryo culture. *J Embryol Exp Morphol* **53,** 75-90.

Wee, E. L., and Zimmerman, E. F. (1980). Palate morphogenesis II: Contraction of cytoplasmic processes in ATP-induced palate rotation in glycerinated mouse heads. *Teratology* **21,** 15-27.

Wilkinson, D. (1989). Homeobox genes and development of the vertebrate CNS. *Bioessays* **10,** 82-85.

Wilkinson, D. G. (1995). Genetic control of segmentation in the vertebrate hindbrain. *Perspect. Dev.Neurobiol.* **3,** 29-38.

Wilkinson, D. G., Bhatt, S., Chavrier, P., Bravo, R., and Charnay, P. (1989). Segment-specific expression of a zinc finger gene in the developing nervous system of the mouse. *Nature* **337,** 187-196.

Winograd, J., Reilly, M. P., Roe, R., Lutz, J., Laughner, E., Xu, X., Hu, L., Asakura, T., Van der Kolk, C., and Strandberg, J. D. (1997). Perinatal lethality and multiple craniofacial malformations in MSX2 transgenic mice. *Hum. Mol. Genet.* **6,** 369-379.

Wintgate, R., and Lumsden, A. (1996). Persistence of rhombomeric organisation in the postsegmental avian hindbrain. *Development* **122,** 2143-2152.

Wood, P. J., and Kraus, B. S. (1962). Prenatal development of the human palate. *Arch Oral Biol.* **7,** 137-150.

Wragg, L. E., Smith, J. A., and Borden, C. S. (1972). Myoneural maturation and function of the foetal rat tongue at the time of secondary palate closure. *Arch Oral Biol.* **17,** 673-682.

Yoshida, H., Kong, Y. Y., Yoshida, R., Elia, A. J., Hakem, A., Hakem, R., Penninger, J. M., and Mak, T. W. (1998). Apaf1 is required for mitochondrial pathways of apoptosis and brain development. *Cell* **94,** 739-750.

Zhang, W., (2003). Temporal and spatial expression of Hoxa2 gene in the developing mouse palate and the effects of valproic acid on Hoxa2 expression during murine palatogenesis. *M.Sc. Thesis*, University of Saskatchewan.

Zhang, Z., Song, Y., Zhao, X., Zhang, X., Fermin, C., and Chen, Y. P. (2002). Rescue of cleft palate in Msx1-deficient mice by transgenic Bmp4 reveals a network pf BMP and Shh signaling in the regulation of mammalian palatogenesis. *Development* **129,** 4135-4146.

Zimmerman, E. F. (1979). Palate morphogenesis: role fo contractile proteins and neurotransmitters. *Advances in the Study of Birth Defects: Abnormal embryogenesis, cellular and molecular aspects* **3,** 143-159.

APPENDIX

pLEGFP-C1 Vector

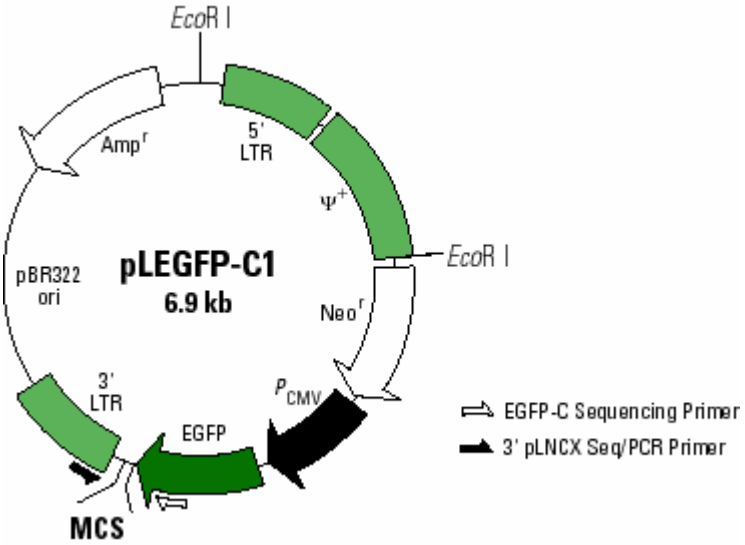

The sequence of *Hoxa2* sense

Sense: (vector primer 1)

GNCCNACGCCGTCNGGATCACTCTCGGCATGGACGAGCTGTACAAGTCCGGA
CTCAGATCTCGAGCC**ATG**AATTACGAATTTGAGCGAGAGATTGGTTTTATCA
ATAGCCAGCCGTCGCTCGCTGAGTGCCTGACATCTTTTCCCCCTGTCGCTGAT
ACATTTCAAAGTTCATCAATCAAGACCTCGACGCTTTCACACTCGACACTGAT
TCCTCCTCCTTTTGAGCAGACCATTCCCAGCCTGAACCCGGGCAGTCACCCTC
GCCACGGCGCTGGCGTTGGCGGCCGCCCCAAGTCGAGCCCCGCGGGCAGTCG
CGGCAGCCCGGTGCCTGCCGGCGCCCTGCAGCCGCCTGAGTATCCCTGGATG
AAGGAGAAGAAGGCGGCCAAGAAAACCGCGCTGCCGCCCGCCGCCGCCTCC
ACGGGCCCTGCCTGCCTCGGCCACAAAGAATCCCTGGAAATAGCTGATGGCA
GCGGCGGGGGATCCAGGCGTCTGAGAACCGCGTACACCAACACTCAGCTTTT
GGAGCTGGAAAAGGAATTTCATTTCAACAAGTACCTTTGCAGACCCGCAGGG
TGGAAATCGCCGCGCTGCTGGATTTGACCGAGAGACAAGTGAAAGTGTGGTT
TCAGAACCGGAGAATGAAGCATAAGAGGCAAACCCAGTGCAAGGAGAACCA
AAACAGCGAAGGGAAATTTAAAAACCTGGAGGACTCGGACAAAGTGGAGGA
AGACGAGGAAGAGAGTCCTCTTTGACAAGCCTCAGTGTCTCCGGGGNCCNTT
TGGAAAGGGNAGGGTACACNTTTCAGCAAAATGGGCTTTCTCAACAGGANGG
CTCCCAATGGAAACNATGGGGAATTCCCNAACTTTTCCAGT

Sense: (vector primer 2)

HindIII

CCCTNTCTCAGACTAAATAAAATCTTTTATTTTATCGATGTTAGGCCATTAAG
GGATCAGTTATCTAGATCCGGTGGATCCCGGGCCCGCGGTACCGTCGACTGC
AGAA**TTCGAA**GCTT**TTA**GTAATTCAGATGCTGTAGGTCGATTGTGGTGAGTG
TGTCTGTAAAAAAGTCAAAGCTGTCAGCTGAGATATCTACAGGACTGTCCAG
GGAGCCAGGCAAGCTGGGCGACAGTGCATCTGAAAGCTGCAGGCAGGAATC
TGTGGAGAAAACATTGAAGTCCTGCAAAGAGGGGACCTCGATGGCCTCGGGA
CTGTCATTGTTTAGGCCAGCTCCACAGTTCTGGCCCATTGTTGACAAGCAGTT
AGGAACAGTGGGTGACTGGTGCTGAAAATGTTTCAAATTTTTCTCATTGCTGG
TTAAAGGCGAAACTGGGAAAGTTTGGGAGTCGCCATTGTGTCCATTGGGAGC
CTGCTGTTGAGAGAGCGCATTTTGCTGAAAAGTGTACCCTTCCCTCTCCAGAA
GGGCCCCGGAGACACTGAGGGCTTGCTCAAAGAGTGACTTCTCTTCCTCGTCT
TCCTCCACTTTGTCCGAGTCCTCCAGGTTTTTAAATTTCCCTTCGCTGTTTTGG
TTCTCCTTGCACTGGGTTTGCCTCTTATGCTTCATTCTCCGGTTCTGAAACCAC
ACTTTCACTTGTCTCTCGGTCAAATCCAGCAGCGCGGCGATTTCCACCCTGCG
GGGTCTGCNAAGGTACTTGNTGAAATGAAATTNCTTTTCCAGCTNCAAAACT
GANTGGTGGTGTACGCGGNTCTCANANGCCTGGATCCCCGCCGCTGCCATCA
GCTATTTCCAGGGATTCTTTGT

The sequence of *Hoxa2* antisense

Antisense: (vector primer 1)

XhoI

TCCAATCNGAATTCNCTCGGCATGGACGAGCTGTACAAGTCCGGACTCAGAT
CTCGAGGAGCTTTGTTTTGCTTTAATGTTC**TTA**GTAATTCAGATGCTGTAGGT
CGATTGTGGTGAGTGTGTCTGTAAAAAAGTCAAAGCTGTCAGCTGAGATATC
TACAGGACTGTCCAGGGAGCCAGGCAAGCTGGGCGACAGTGCATCTGAAAG
CTGCAGGCAGGAATCTGTGGAGAAAACATTGAAGTCCTGCAAAGAGGGGAC
CTCGATGGCCTCGGGACTGTCATTGTTTAGGCCAGCTCCACAGTTCTGGCCCA
TTGTTGACAAGCAGTTAGGAACAGTGGGTGACTGGTGCTGAAAATGTTTCAA
ATTTTTCTCATTGCTGGTTAAAGGCGAAACTGGGAAAGTTTGGGAGTCGCCAT
TGTGTCCATTGGGAGCCTGCTGTTGAGAGAGCGCATTTTGCTGAAAAGTGTAC
CCTTCCCTCTCCAGAAGGGCCCCGGAGACACTGAGGGCTTGCTCAAAGAGTG
ACTTCTCTTCCTCGTCTTCCTCCACTTTGTCCGAGTCCTCCAGGTTTTTAAATT
TCCCTTCGCTGTTTTGGTTCTCCTTGCACTGGGTTTGCCTCTTATGCTTCATTCT
CCGGTTCTGAAACCACACTTTCACTTGTCTCTCGGTCAAATCCAGCAGCGCGG
CGATTTCCACCCTGCGGGGTCTGCAAAGGTACTTGTTGAAATGAAATTCCTTT
TCCAGCTCCNAAANCTGANTGTTGGTGTACGCGGTTCTCANACGCCTGGGAT
CCCCCGCCGCTGNCATCAGCTATTTTCAGGGATTCTTTGTGGGCCNAAGCAGG
CANGGCCCCTGGAAGCGGCCGCCG

Figure **EGFP expression after transfection with pLEGFP vector (10X)**

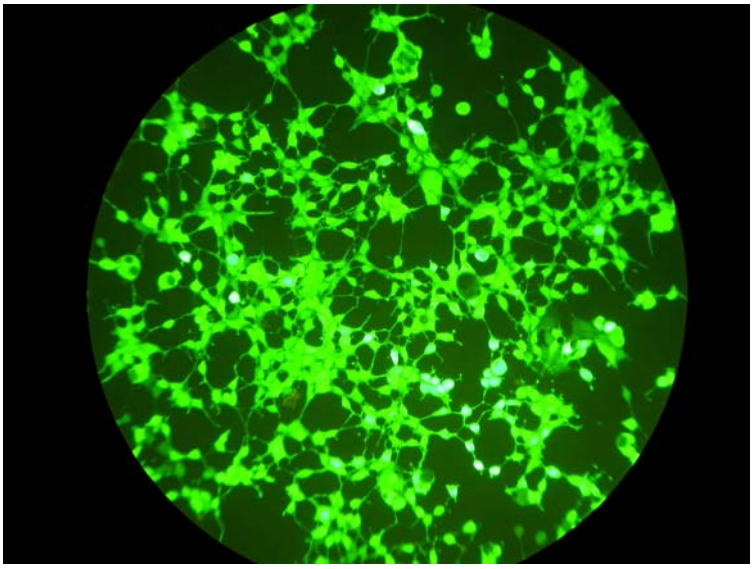

Table **Fusion effects of *Hoxa2* gene on cultured fetal mouse palates in different genotypes** (Data obtained from *Zhang, W., M.Sc. Thesis, 2003*)

Types of mouse embryos	Frequency of fused palates (FFP)	Frequency of contacted palates (±fusion)
Wild-type	90.0% (18/20)	100% *(20/20)
Heterozygous	78.7% (37/47)	85.1% (40/47)
Mutant	44.4% (8/18)	72.2% (13/18)